

Reference

NBS
PUBLICATIONS

NAT'L INST. OF STAND & TECH
A11106 340351



NBS TECHNICAL NOTE 1081

U.S. DEPARTMENT OF COMMERCE / National Bureau of Standards

Possible Estimation Methodologies for Electromagnetic Field Distributions in Complex Environments

M. Kanda
J. Randa
N. S. Nahman

-QC
100
.U5753
No.1081
1985

NATIONAL BUREAU OF STANDARDS

The National Bureau of Standards¹ was established by an act of Congress on March 3, 1901. The Bureau's overall goal is to strengthen and advance the Nation's science and technology and facilitate their effective application for public benefit. To this end, the Bureau conducts research and provides: (1) a basis for the Nation's physical measurement system, (2) scientific and technological services for industry and government, (3) a technical basis for equity in trade, and (4) technical services to promote public safety. The Bureau's technical work is performed by the National Measurement Laboratory, the National Engineering Laboratory, and the Institute for Computer Sciences and Technology.

THE NATIONAL MEASUREMENT LABORATORY provides the national system of physical and chemical and materials measurement; coordinates the system with measurement systems of other nations and furnishes essential services leading to accurate and uniform physical and chemical measurement throughout the Nation's scientific community, industry, and commerce; conducts materials research leading to improved methods of measurement, standards, and data on the properties of materials needed by industry, commerce, educational institutions, and Government; provides advisory and research services to other Government agencies; develops, produces, and distributes Standard Reference Materials; and provides calibration services. The Laboratory consists of the following centers:

Absolute Physical Quantities² — Radiation Research — Chemical Physics —
Analytical Chemistry — Materials Science

THE NATIONAL ENGINEERING LABORATORY provides technology and technical services to the public and private sectors to address national needs and to solve national problems; conducts research in engineering and applied science in support of these efforts; builds and maintains competence in the necessary disciplines required to carry out this research and technical service; develops engineering data and measurement capabilities; provides engineering measurement traceability services; develops test methods and proposes engineering standards and code changes; develops and proposes new engineering practices; and develops and improves mechanisms to transfer results of its research to the ultimate user. The Laboratory consists of the following centers:

Applied Mathematics — Electronics and Electrical Engineering² — Manufacturing
Engineering — Building Technology — Fire Research — Chemical Engineering²

THE INSTITUTE FOR COMPUTER SCIENCES AND TECHNOLOGY conducts research and provides scientific and technical services to aid Federal agencies in the selection, acquisition, application, and use of computer technology to improve effectiveness and economy in Government operations in accordance with Public Law 89-306 (40 U.S.C. 759), relevant Executive Orders, and other directives; carries out this mission by managing the Federal Information Processing Standards Program, developing Federal ADP standards guidelines, and managing Federal participation in ADP voluntary standardization activities; provides scientific and technological advisory services and assistance to Federal agencies; and provides the technical foundation for computer-related policies of the Federal Government. The Institute consists of the following centers:

Programming Science and Technology — Computer Systems Engineering.

¹Headquarters and Laboratories at Gaithersburg, MD, unless otherwise noted;
mailing address Washington, DC 20234.

²Some divisions within the center are located at Boulder, CO 80303.

Possible Estimation Methodologies for Electromagnetic Field Distributions in Complex Environments

M. Kanda
J. Randa
N. S. Nahman

Electromagnetic Fields Division
National Engineering Laboratory
National Bureau of Standards
U.S. Department of Commerce
Boulder, Colorado 80303



NBS technical note

U.S. DEPARTMENT OF COMMERCE, Malcolm Baldrige, Secretary

NATIONAL BUREAU OF STANDARDS, Ernest Ambler, Director

Issued March 1985

National Bureau of Standards Technical Note 1081
Natl. Bur. Stand. (U.S.), Tech Note 1081, 52 pages (Mar. 1985)
CODEN: NBTNAE

U.S. GOVERNMENT PRINTING OFFICE
WASHINGTON: 1985

CONTENTS

	Page
1. Introduction.....	1
2. Statistical Approach.....	2
2.1 Rayleigh Distribution.....	2
2.2 Examples.....	5
2.3 Other Relevant Statistics.....	6
3. Finite-Element Action Approach.....	8
3.1 Introduction and Motivation.....	8
3.2 General Formulation.....	11
3.3 Simple Example.....	14
3.4 Problems and Prospects.....	19
4. Scanning Techniques.....	21
4.1 Cylindrical Scanning.....	21
4.2 Spherical (Directional) Scanning.....	26
5. Summary.....	29
6. References.....	30
Appendix.....	31

Possible Estimation Methodologies for Electromagnetic Field Distributions in Complex Environments

M. Kanda, J. Randa, and N. S. Nahman
Electromagnetic Fields Division
National Bureau of Standards
Boulder, Colorado 80303

The problem of measuring and characterizing complicated multiple-source, multiple-frequency electromagnetic environments is becoming more important and more difficult as electrical devices proliferate. This paper outlines three general approaches to the problem which are currently under investigation at the National Bureau of Standards. The three approaches are: 1) a statistical treatment of the spatial distribution of electromagnetic field intensities, 2) a numerical computation using a finite-element (or lattice) form of the electromagnetic action functional, and 3) use of a directional probe to scan a volume. All three methods are still in the development stage, but each appears promising.

Key words: action, directional scanning, environment characterization, field levels, finite element, hazard assessment, multiple source, statistical approach.

1. Introduction

There has recently been a rapid increase in higher powered, multi-frequency, electromagnetic (EM) radiation sources which complicate greatly the environment in which modern electronic equipment, both military and civilian, must operate. At the same time, there has been an even more dramatic increase in the quantity of electronic equipment, such as minicomputers and microprocessors, composed of semiconductor devices, and hence more sensitive to interference. Today there is a complex matrix of electronic equipment trying to operate in a complex EM environment. Therefore, the estimation of the maximum electromagnetic (EM) field strength is becoming very important in many interference problems. For example, electromagnetic waves penetrate into buildings which house sensitive electronic and ordnance items. There has been great interest in determining the electromagnetic environment inside buildings.

Heretofore, it has been customary to make several spot measurements of the electromagnetic field strengths produced by existing transmitters. However, it is obviously impossible to completely determine the field existing in

an enclosure using a manageable number of spot measurements. In order to rigorously determine the EM field distributions in a volume, systematic measurements of electric field amplitude and phases have to be made at points at most half a wavelength apart (at the highest frequency present).

There is a need for a general method of extracting the maximum amount of useful information about the EM field distribution within an enclosure from the minimum amount of measurement effort. In this paper we discuss three possible approaches to this problem which are currently being explored and developed at the National Bureau of Standards (NBS). We first examine a statistical approach to the estimation of EM field distributions. In a previous paper by the first author [1], five types of time and amplitude statistics were used in order to unravel the complexities involved in an EM environment. Here we shall discuss the statistical distribution of scattered EM fields and illustrate its usefulness using experimental and simulated examples. The second method is a finite-element-action calculation using a small number of measurement points. The true field cannot be determined, but it may be possible to reconstruct the smoothest configuration or the "most probable" one. The third and final approach discussed is the most conventional, using directional scanning to bound or approximately determine fields within a given volume.

2. Statistical Approach

2.1 Rayleigh Distribution

When the configuration of the scatterers is random and sufficiently dispersed to give a wide (and hence, equivalently uniform) phase distribution, the field configuration, E , typically caused by the reflectivity of various multipath types of scatterers, both stationary and moving, is given by

$$E = \sum_{i=1}^N A_i e^{j\phi_i}, \quad (2.1)$$

where A_i and ϕ_i are random amplitudes and phases of scattered fields.

Resolving E into its real and imaginary components, $\text{Re } E$ and $\text{Im } E$, from the central limit theorem, it follows that $\text{Re } E$ and $\text{Im } E$ are normally distributed, as long as N is large (> 10). In particular, when the A_i and ϕ_i are uncor-

related and hence independent random variables, it can be shown that $\text{Re } E$ and $\text{Im } E$ have the same variance with zero mean values. The amplitude distribution $p_E(r)$ is then found to be the Rayleigh distribution [2] $p_E(r) = \frac{r}{\sigma^2} \exp(-\frac{r^2}{2\sigma^2})$ for $r > 0$.

The mean $\langle E \rangle$, mean square $\langle E^2 \rangle$ and standard deviation (s.d.) are respectively given as

$$\langle E \rangle = \int_0^{\infty} r p_E(r) dr = \sqrt{\frac{\pi}{2}} \sigma \quad (2.2)$$

$$\langle E^2 \rangle = 2\sigma^2 \quad (2.3)$$

and

$$\text{s.d.} = \sqrt{\langle E^2 \rangle - \langle E \rangle^2} = \sqrt{2 - \frac{\pi}{2}} \sigma. \quad (2.4)$$

The cumulative probability distribution is defined as the probability that the random variable E is equal or less than the value E_0 , and can be obtained by integrating the Rayleigh probability density function, i.e.,

$$P(E < E_0) = \int_0^{E_0} \frac{r}{\sigma^2} \exp(-\frac{r^2}{2\sigma^2}) dr = 1 - \exp(-\frac{E_0^2}{2\sigma^2}). \quad (2.5)$$

Hence, its complement is

$$p(E > E_0) = \exp(-\frac{E_0^2}{2\sigma^2}) \quad (2.6)$$

The median of E , E_m , is, therefore,

$$P(E < E_m) = 1 - \exp(-\frac{E_m^2}{2\sigma^2}) = 0.5 \quad (2.7)$$

or

$$E_m \cong 1.18 \sigma. \quad (2.8)$$

The average crossing rate (ACR) presents the average number of times the EM field strength crosses various levels and is usually given as positive crossing per second versus EM field strength. The average level crossing rate at a given level E_0 is [3]

$$\bar{n}(E = E_0) = \int_0^{\infty} \dot{r} p_E(E_0; \dot{r}) d\dot{r} \quad (2.9)$$

where $p_E(E_0, \dot{r})$ is the joint probability distribution of E , and $\dot{r} = \frac{dr}{dt}$ gives the slope of the signal envelope E . For the case of the Rayleigh distribution, the level crossing rate becomes

$$\bar{n}(E = E_0) = \frac{v}{\sqrt{2\pi}} \frac{E_0}{\sigma^2} \exp\left(-\frac{E_0^2}{2\sigma^2}\right) \quad (2.10)$$

where*

$$v^2 = \langle \dot{E}^2 \rangle . \quad (2.11)$$

The average field strength can be determined by averaging the random trial samples of instantaneous field strength measurements recorded over a certain path length in distance. The variation in the average field strength is typically caused by the relatively small scale variations along the propagation path.

There are situations where a signal is received in two different ways, one via many widely spaced scatterers or reflectors, the other by a quite different mechanism, e.g., directly from a transmitter. The analysis of the amplitude distribution of the resultant signal can be achieved as follows. Consider the sum

$$E = A_0 e^{j\phi_0} + \sum_{i=1}^N A_i e^{j\phi_i} . \quad (2.12)$$

The first term represents the direct-path propagation through the walls of houses and other objects. The second term represents the reflected and scattered waves due to randomly oriented objects such as houses, buildings, walls, and overhead wires, and is therefore, Rayleigh distributed. Since the direct-path propagation is attenuated through each penetration of a wall, etc., the amplitude of this direct wave will be

$$A_0 \propto \exp \left[- \sum_{i=1}^M \delta_i d_i \right] \quad (2.13)$$

where d_i is the thickness and δ_i is the attenuation constant of each of the walls. When M is large, the central limit theorem indicated that the sum of the random term $\delta_i d_i$ will be normally distributed. Hence, the amplitude distribution of A_0 is lognormal, i.e.,

$$p_{A_0}(r) = \frac{1}{r \alpha \sqrt{2\pi}} \exp\left[-\frac{(\ln r - \mu)^2}{2\alpha^2}\right] \quad (2.14)$$

where μ is the mean and α^2 is the variance of the exponent in eq (2.13).

The probability density function of the total field given by the sum of a random plus a Rayleigh phasor is [2]

$$p(r) = \frac{2r}{\alpha \sigma \sqrt{2\pi}} \int_0^\infty A_0^{-1} \exp\left[-\frac{(\ln A_0 - \mu)^2}{2\alpha^2} - \frac{r^2 + A_0^2}{\sigma}\right] \cdot I_0\left(\frac{2r A_0}{\sigma}\right) dA_0 \quad (2.15)$$

where α is the mean-square value of the scattered components.

For the cases of large and small values of E,

$$p_E(r) = \begin{cases} \frac{1}{r \alpha \sqrt{2\pi}} \exp\left[-\frac{(\ln r - \mu)^2}{2\alpha^2}\right] & \text{for } r > \sqrt{2}\sigma \\ \frac{r}{\sigma^2} \exp(-r^2/2\sigma^2) & \text{for } r < \sqrt{2}\sigma \end{cases} \quad (2.16)$$

$$\quad (2.17)$$

where μ is the mean and σ^2 is the variance of E.

Equations (2.16, 2.17) indicate that E is lognormal for large values and Rayleigh distributed for small values.

The Rayleigh distribution has one parameter σ to be determined which follows simply from the estimated mean $\hat{\sigma}$ given as

$$\hat{\mu} = \frac{1}{N} \sum_{i=1}^N E_i, \quad (2.18)$$

and therefore

$$\hat{\sigma} = \sqrt{\frac{2}{\pi}} \hat{\mu}. \quad (2.19)$$

2.2. Examples

A number of electromagnetic field measurements have been made on the propagation of radio waves at VHF and higher frequencies in the presence of buildings, trees and other obstacles [1,4,5,6]. As an example, the cumulative amplitude probability distribution and the average crossing rate of the EM noise measured in a coal mine [1] are shown in figures 2-1 and 2-2,

respectively. Figure 2-1 indicates that, when the field strength is low (approximately 90% of the total sample), the Rayleigh distribution is a good approximation of the EM noise in a mine. On the other hand, when the EM field strength is high (less than 10% of the total sample), EM noise data show a departure from the Rayleigh distribution. The statistical properties of the peak values of EM field may be close to the log-normal distribution as indicated in eq (2.16).

Measurements of attenuation due to buildings, trees, and other obstacles at long propagation distances (e.g., ranging from 100 to 500 m for 800 MHz propagation), have also been performed [6]. As an example, figure 2-3 shows the cumulative amplitude probability distribution of the attenuation data. A straight line on the coordinates in figure 2-3 represents a log-normal distribution of signal levels. The measured distribution is approximated by a log-normal distribution which is discussed in eq (2.16).

To simulate these experimental results, numerical studies of the cumulative amplitude probability distribution for a two-dimensional cavity model with random noise sources have been made [7]. Figure 2-4 shows the cumulative amplitude probability distribution for EM fields measured inside the rectangular cavity. This figure is obtained from 100 data sets which are generated by using random noise source positions and random wavelengths. The results follow a lognormal distribution except for the low probability region where most electromagnetic interference data show a departure from a lognormal distribution. The deviation from a lognormal distribution in the low probability region indicates an accurate estimation of the maximum field strength for the measured data may be very difficult.

2.3 Other Relevant Statistics

In its most general form the characterization of a stationary electromagnetic environment is based on observations of a three-dimensional, random variable. As such, the electromagnetic field is represented by the electric and magnetic field vectors \vec{E} and \vec{H} , respectively, where both of these vectors may be stationary random functions of their spatial coordinates.

If the field vectors are not stationary, the probability distributions of

the electromagnetic field vectors are dependent upon time. The process required for the environment to change from one stationary state to another is defined as the transient state and is not considered here.

For stationary electromagnetic excitation the applied fields or sources whose collective effects establish the EM environment within a volume are defined here as steady-state fields. Thus, the random nature of the field is established by the random spatial distribution of the sources, and the random boundaries of objects within the volume or the randomness of the boundary itself.

There are various statistical approaches which may be useful for characterizing this class of electromagnetic environments; two approaches are previously discussed; i.e., cumulative probability distribution and averaging crossing rate.

Three other approaches are mentioned here as having possible merit.

A. Interpulse Spacing Distribution

The interpulse spacing distributions give the probability distribution for the spacing between successive pulses in the received noise process. These distributions are, of course, functions of the noise amplitude level.

B. Pulse Duration Distribution

The pulse duration distributions give the probability distribution for the pulse widths and are given in terms of the percentage of pulses which exceed various widths in seconds.

C. Two Sample Variance Analysis

It is essential to know how much data to gather when dealing with statistical quantities. Therefore, in any measurement of a statistical phenomenon the minimum length of time over which the phenomenon is observed should be determined. Two sample variance analysis can be used to accomplish this determination. The basic idea to be discussed briefly below has been implemented often in the discussion of frequency stability.

A record of the phenomenon under consideration, $y(t)$, is divided into a number of equal time segments of length τ , and the average value of $y(t)$, y_k , of each segment is calculated by

$$y_k = \frac{1}{\tau} \int_{t_k}^{t_k + \tau} y(t) dt, \quad (2.20)$$

where y_k is the k^{th} segment average starting at time t_k . Next, the sample variance (sample size two) $\sigma_k^2(2, \tau)$, of successive averages is calculated. That is

$$\sigma_k^2(2, \tau) = \frac{\sum_{n=k}^{k+1} (y_n - \bar{y}_k)^2}{2} = \frac{1}{2} (y_{k+1} - y_k)^2, \quad (2.21)$$

where

$$\bar{y}_k \equiv \frac{1}{2} \sum_{n=k}^{k+1} y_n \quad (2.22)$$

is the average of the two successive segment averages y_k and y_{k+1} . The two sample variance, $\sigma_y^2(2, \tau)$, for this special case (sample size two) is then defined to be

$$\sigma_y^2(2, \tau) \equiv \langle \sigma_k^2(2, \tau) \rangle, \quad (2.23)$$

where the brackets represent the average of $\sigma_k^2(2, \tau)$ over all pairs of successive y_k constructed from $y(t)$. The preceding calculation is repeated for various values of averaging period, τ . For a given maximum allowable deviation in $y(t)$ the minimum averaging time can then be determined.

Many examples of these time and amplitude statistics for the time dependent, EM noise are given elsewhere [1].

3. Finite-Element Action Approach

3.1 Introduction and Motivation

In this section we describe an approach which in effect attempts to solve Maxwell's equations within the volume of interest. The type of problem in which we are interested, however, differs fundamentally from those problems for which Maxwell's equations are usually solved, and it resists the use of standard methods. The most fundamental difference is that we do not know the

sources. In addition there are the complications that the geometry and the time dependence are not simple. The information available includes boundary conditions at conducting walls or dielectric interfaces within the volume, and the measured values of the fields at some number of measurement points. We are free to specify the number and location of the measurement points, but we obviously want the number to be small--or at least "reasonable." The general qualitative idea is that given the geometry and boundary conditions, knowledge of the fields at a few points should enable one to extract some information about global properties such as average or maximum electromagnetic energy density.

Without knowledge of the external sources radiating into the volume of interest, and with only a few measurement points, there will not in general be a unique solution to Maxwell's equations. Consequently, it will be impossible to actually determine the field everywhere. The best one can hope for is that the approximate values and positions of the maximum field intensities will be the same for all allowed solutions. Failing that, one wants a method which consistently finds the one solution of all those possible which has some property of interest, such as the smallest maximum power density.

An approach which appears to hold some promise of fulfilling these rather demanding (perhaps impossible) requirements is based on a finite-element treatment of Hamilton's principle applied to electrodynamics. For a classical field theory, Hamilton's principle states that if one considers the quantity

$$S[\psi^\alpha] = \int_{t_1}^{t_2} dt \int d^3x \mathcal{L}(\psi^\alpha(\vec{x}, t)), \quad (3.1)$$

where $\mathcal{L}(\psi^\alpha)$ is the Lagrangian density of the system depending on the independent fields $\psi^\alpha(\vec{x}, t)$, then the values assumed by the fields for the correct physical solution are such that S is stationary with respect to small variations of the fields, $\psi^\alpha(\vec{x}, t)$. The functional $S[\psi^\alpha]$ is called the action, and for electrodynamics the stationarity requirement yields Maxwell's equations [8], as we shall outline in the next subsection. It is generally assumed that the stationary point of the action is in fact a minimum, and general conditions are known for which this is so [9]. Unfortunately, these conditions are generally not met in the cases of interest to us, and so finding the

stationary point of S is not necessarily as "simple" as minimizing it. This will be discussed further in a later subsection.

Finite-element calculations minimizing the action have been used before in electromagnetics, particularly for waveguide and cavity problems [10,11], and the connection to other variational calculations has been pointed out [11]. Previous approaches, however, have obtained a set of linear equations by using finite elements and setting the appropriate derivatives equal to zero. The system was then solved by numerically inverting the matrix. Such tactics will not work here because there is not a unique solution, and hence the matrix would be (very) singular. Our preference is to work directly with the action and search numerically for its stationary points, rather than working with its derivatives. This approach is probably closer in spirit to methods currently popular in quantum field theory [12] than to the traditional differential equations approach.

In the finite-element approach we replace the continuous variables \bar{x} and t by a four-dimensional grid of points on which the fields are defined. The integral in the action then becomes a sum, and the field values at each (unmeasured) point are varied until a stationary point of the action is found. The field values at measurement points are set equal to their measured values and not allowed to vary. When a stationary point is found, one has a solution of Maxwell's equations for which the fields take on their measured values at measurement points. Which of the many possible such solutions one finds will depend on the initial field configuration (before we vary the fields) and on the method used to find the stationary point. In the present work we are using a smooth starting configuration and a gradient "minimization" procedure, which should find the solution which has the smoothest field configuration.

The remainder of this section is devoted to a more detailed account of the progress made in formulating this approach and the (foreseeable) remaining problems. We shall first present the general framework, then digress on the question of whether the stationary point is a minimum. Next a simple example is given, and finally we discuss remaining obstacles and the direction of future work.

3.2 General Formulation

The action for electromagnetism is given by [8]

$$\begin{aligned}
 S[\bar{A}, \phi] = & \int_{t_1}^{t_2} dt \int d^3x \left\{ \frac{1}{2} (\bar{\nabla}\phi(\bar{x},t) + \frac{\partial}{\partial t} \bar{A}(\bar{x},t)) \cdot \bar{\epsilon}(\bar{x},t) \cdot (\bar{\nabla}\phi(\bar{x},t) \right. \\
 & + \frac{\partial}{\partial t} \bar{A}(\bar{x},t)) - (\bar{\nabla} \times \bar{A}(\bar{x},t)) \cdot \bar{\mu}^{-1}(\bar{x},t) \cdot (\bar{\nabla} \times \bar{A}(\bar{x},t))] \\
 & \left. + \bar{A}(\bar{x},t) \cdot \bar{J}(\bar{x},t) - \rho(\bar{x},t) \phi(\bar{x},t) \right\} , \tag{3.2}
 \end{aligned}$$

where we have assumed all media are lossless, and $\bar{\epsilon}$ and $\bar{\mu}$ are the permittivity and permeability tensors. \bar{A} and ϕ are the usual vector and scalar potentials,

$$\bar{E}(\bar{x},t) = -\bar{\nabla}\phi - \frac{\partial}{\partial t} \bar{A} \quad , \quad \bar{B}(\bar{x},t) = \bar{\nabla} \times \bar{A} \quad . \tag{3.3}$$

The time integral in eq (3.2) is typically taken from $-\infty$ to $+\infty$, and similarly the volume integral usually extends over all space--although one can also consider a finite volume or time range, subject to conditions we shall note below. \bar{J} and ρ are the current and charge densities respectively. We have written the action in terms of the potentials rather than \bar{E} and \bar{H} , because in varying the action we want to take variations only with respect to independent variables, whereas \bar{E} and \bar{H} are related through eq (3.3). In fact, eq (3.3) implies the two homogeneous Maxwell's equations,

$$\bar{\nabla} \cdot \bar{B} = 0 \quad , \quad \bar{\nabla} \times \bar{E} + \frac{\partial}{\partial t} \bar{B} = 0 \quad . \tag{3.4}$$

Although there are four independent potential functions (\bar{A}, ϕ) appearing in eq (3.2), only three are independent, since the gauge choice will provide an extra relation.

If one considers variation of the action due to a small variation of $\phi(\bar{x},t)$ ($\delta\phi(\bar{x},t)$) one finds (assuming the permittivity tensor is symmetric)

$$\delta_{\phi} S = - \int_{t_1}^{t_2} dt \int_S d^2x \hat{n} \cdot \bar{D} \delta\phi(\bar{x},t) + \int_{t_1}^{t_2} dt \int d^3x (\bar{\nabla} \cdot \bar{D} - \rho) \delta\phi, \quad (3.5)$$

$$\bar{D} = \bar{\epsilon} \cdot \left(-\bar{\nabla}\phi - \frac{\partial}{\partial t} \bar{A} \right),$$

where the surface integral is over the surface enclosing the entire volume. If we require that ϕ not vary on the boundary surface, but otherwise let $\delta\phi(\bar{x},t)$ be arbitrary, then the first term in eq (3.5) vanishes, and requiring that the action be stationary yields

$$\delta_{\phi} S = \int_{t_1}^{t_2} dt \int d^3x (\bar{\nabla} \cdot \bar{D} - \rho) \delta\phi = 0 \quad (3.6)$$

$$\rightarrow \bar{\nabla} \cdot \bar{D}(\bar{x},t) - \rho(\bar{x},t) = 0 .$$

In a similar manner, requiring that S be stationary with respect to small variations of $\bar{A}(\bar{x},t)$ leads to

$$\delta_A S = 0 \rightarrow \frac{\partial}{\partial t} \bar{D} - \bar{\nabla} \times \bar{H} + \bar{J} = 0 , \quad (3.7)$$

where $\bar{A}(\bar{x},t)$ must be held fixed not only on the boundary surface at all times but also throughout the volume at times t_1 and t_2 . What this means in practice is that in order to use this in a calculation, one must specify the fields on the boundary surface at all times and throughout the volume at the initial and final times. In any real application, such a superabundance of information will not be available for the volume of interest. In order to exploit the stationarity of the action we must expand the volume considered beyond just the region of interest, out to distances where the fields can be assumed to be negligible. The same applies to the time; t_1 is chosen before the fields are turned on and t_2 after they are turned off.

Having extended the volume under consideration to virtually all of space-time, we must restrict the problem to manageable size. We envision the division depicted in figure 3-1. The volume marked V_I is the region of interest; it is assumed to be free of primary sources, but it may contain conductors with induced currents. Volume V_B is a buffer zone between V_I and V_S , which is the rest of space, wherein are located any primary sources. The general idea

is to divide the action into one piece from the integral over volumes V_I and V_B and another piece from V_S . Because V_S contains unknown sources, we do not try to determine the fields there, which means that we also will not know the fields on the surface between V_S and V_B . The fields on that surface will be allowed to vary or will be fixed by a reasonable guess. Obviously, near the boundary between V_S and V_B the solution obtained will be very sensitive to the choice for the fields on that boundary, and therefore it will not be reliable. As one moves away from the outer boundary of V_B the values of the fields should be influenced more by the measurement points and less by the values on the surface between V_S and V_B . For points far enough away from that surface--i.e. within V_I --it should be possible to obtain reliable solutions, given enough measurement points. The hope is that "far enough away" and "enough points" are not so large as to render the method impractical for most applications. The positions of the measurement points will clearly affect the size required for V_B ; it may well be advantageous to make a few measurements on the perimeter of V_B . It would probably also be advisable to choose the boundary of V_B to coincide with conducting walls when it is feasible, in order to constrain the fields on the boundary as much as possible.

The quantity we shall consider then is a reduced action, \hat{S} , which is defined as in eq (3.2) but with the integral restricted to $V_I + V_B$. (Note that in the general multiple-frequency case the various volumes are four-dimensional space-time volumes.) For definiteness and simplicity we choose a gauge which will be used in the remainder of the section. The choice is $\phi(\vec{x},t) = 0$, so that $\vec{E} = -\partial\vec{A}/\partial t$. The next step is to discretize the expression for the reduced action, converting the volume integral into a summation which approximates it. There are any number of ways to do so; we are not interested in their relative (dis)advantages at this time. The discretized reduced action will have the general form

$$\hat{S} = \int dt \sum_{\alpha, \beta, \gamma \in V_I \oplus V_B} \Delta V_{\alpha\beta\gamma} \left\{ \frac{1}{2} \left(\frac{\partial}{\partial t} \bar{A}(t) \right)_{\alpha\beta\gamma} \cdot \bar{\epsilon}_{\alpha\beta\gamma} \cdot \left(\frac{\partial}{\partial t} \bar{A}(t) \right)_{\alpha\beta\gamma} - \left(\bar{\nabla} \times \bar{A}(t) \right)_{\alpha\beta\gamma} \cdot \bar{\mu}^{-1}_{\alpha\beta\gamma} \cdot \left(\bar{\nabla} \times \bar{A}(t) \right)_{\alpha\beta\gamma} \right\}, \quad (3.8)$$

where a number of points require explanatory comment. The discrete indices α, β, γ label the spatial points, on which are centered the volume elements

$\Delta V_{\alpha\beta\gamma}$. We have left the time variable continuous for now, anticipating the single-frequency example below, Section (3.3), but for the general case time too would be made discrete. The quantities $(\partial A/\partial t)_{\alpha\beta\gamma}$ and $(\bar{\nabla} \times \bar{A})_{\alpha\beta\gamma}$ will in general depend on the values of the field \bar{A} at a number of points on (or within) the surface bounding $\Delta V_{\alpha\beta\gamma}$. A concrete realization of this discretization of \hat{S} will be given in the example below. Imposition of the constraints required by the known values of \bar{E} and/or \bar{H} at measurement points can be rather complicated, but a simple case illustrates the idea. If only one frequency is present then for our gauge choice $\bar{E}_{\alpha\beta\gamma} \propto \bar{A}_{\alpha\beta\gamma}$, and a measurement of the electric field at a point fixes $\bar{A}_{\alpha\beta\gamma}$ at that point. A similar comment applies to boundary conditions at perfectly conducting walls; for the single-frequency case they can be imposed with relative ease.

The calculation then proceeds as follows. A grid is defined within $V_B \oplus V_I$, and $\bar{A}_{\alpha\beta\gamma}$ is fixed at measurement points and appropriate components are set equal to zero at conducting walls. All other $\bar{A}_{\alpha\beta\gamma}$'s are varied, and one searches numerically for a stationary point of \hat{S} in eq (3.8). When (if) a stationary point is found, then that set of $\bar{A}_{\alpha\beta\gamma}$ constitutes an approximate solution to Maxwell's equations within $V_B \oplus V_I$ which is consistent with measured field values and boundary conditions. The entire procedure, including the numerical search method, is greatly clarified by an example, to which the next subsection is devoted. The question of whether the stationary point is a maximum, minimum, or neither is addressed in the Appendix.

3.3 Simple Example

Having presented the general ideas of this approach, we now attempt to implement it in a simple example--a rectangular waveguide with perfectly conducting walls. This is obviously not supposed to be a practical application, and many of the difficulties and nuances of the general case are absent. It is a practice problem to demonstrate the idea and to provide a basis on which to build toward solution of real problems. The rectangular waveguide is chosen because it has simple known solutions, because the boundary conditions are easily imposed, and because it reduces to a two-dimensional problem, thereby reducing the computational exercise.

We continue to use the $\phi(\bar{x},t) = 0$ gauge. The known time and longitudinal dependence are imposed by writing the vector potential and current induced in the walls as

$$\begin{aligned}\bar{A}(\bar{x},t) &= \bar{A}(\bar{x}_\perp) \cos(\omega t - kz) \equiv \bar{A}(\perp) \cos(\omega t - kz), \\ \bar{J}(\bar{x},t) &= \bar{J}(\perp) \cos(\omega t - kz), \quad k = \sqrt{\frac{\omega^2}{c^2} - \frac{\pi^2}{a^2}},\end{aligned}\tag{3.9}$$

where c is the speed of light in the waveguide medium, $\bar{x}_\perp = (x,y)$ is the two-dimensional transverse position vector, and where $\bar{A}(\bar{x},t)$ and $\bar{A}(\perp)$ are real. Substitution of eq (3.9) in eq (3.2) yields

$$\begin{aligned}S &= C \int_{-\Delta}^{a+\Delta} dx \int_{-\Delta}^{b+\Delta} dy \left\{ \frac{\pi^2}{a^2} [A_y^2(\perp) + A_x^2(\perp)] + \frac{\omega^2}{c^2} A_z^2(\perp) \right. \\ &\quad - [(\partial_y A_z(\perp))^2 + (\partial_x A_z(\perp))^2 + (\partial_x A_y(\perp) - \partial_y A_x(\perp))^2] \\ &\quad \left. + 2\mu \bar{J}(\perp) \cdot \bar{A}(\perp) \right\},\end{aligned}\tag{3.10}$$

$$C = \frac{1}{2\mu} \int dt \int dz \cos^2(\omega t - kz) \approx \frac{1}{2\mu} \int dt \int dz \sin^2(\omega t - kz).$$

In writing eq (3.10) we have assumed that the material in the waveguide is isotropic and that the range of the t and/or z integration(s) is either very long or an even number of cycles. The induced current term and the limits of the transverse integrations require explanation. In order that the stationary point of S yield Maxwell's equations, the variations of \bar{A} must be zero on the boundary, which in our two-dimensional case here means that we must specify \bar{A} on the transverse boundary. In order to be able to specify all components of \bar{A} we choose the boundary to lie a few skin depths within the conducting walls where the field can safely be assumed to vanish. Referring to figure 3-2, the x integration goes from $x = -\Delta$ to $x = a + \Delta$, and the y integration from $-\Delta$ to $b + \Delta$, where $\Delta \equiv N\delta$, some suitable number of skin depths. Then, however, the currents induced in the walls are contained within the integration volume. Fortunately, we can show that the contribution to the action from the volume within the conductor is negligible, and we can write

$$S \approx C \int_0^a dx \int_0^b dy \left\{ \frac{\pi^2}{4a^2} [A_y^2(\perp) + A_x^2(\perp)] + \frac{\omega^2}{c^2} A_z^2(\perp) - [(\partial_y A_z(\perp))^2 + (\partial_x A_z(\perp))^2 + (\partial_x' A_y(\perp) - \partial_y A_x(\perp))^2] \right\}. \quad (3.11)$$

We still need to impose $\vec{E}_{\text{tan}} = 0$ and $\vec{B}_{\text{norm}} = 0$ at the conductor walls, which is accomplished by the requirements that

$$A_z(0,y) = A_z(x,0) = A_z(a,y) = A_z(x,b) = 0,$$

$$A_x(x,0) = A_x(x,b) = 0, \quad (3.12)$$

$$A_y(0,y) = A_y(a,y) = 0.$$

The action is then discretized by breaking up the waveguide into a rectangular grid as in figure 3-3, with area elements centered on crosses and field values defined on dots. The spacing between dots is $\Delta x = a/N_x$, $\Delta y = b/N_y$. The field value for an area element is given by the average of the values at the four corners of the element. For derivatives, the average of the two appropriate differences is used, e.g.,

$$\left(\frac{d A_x}{dx} \right) (i+\frac{1}{2}, j+\frac{1}{2}) = \frac{1}{2\Delta x} [A_x(i+1, j+1) - A_x(i, j+1) + A_x(i+1, j) - A_x(i, j)]. \quad (3.13)$$

The action then takes the form

$$S \approx C \Delta x \Delta y \sum_{\alpha=1}^{N_x} \sum_{\beta=1}^{N_y} \left\{ \left(\frac{\pi}{4a} \right)^2 [A_y(\alpha, \beta) + A_y(\alpha-1, \beta) + A_y(\alpha, \beta-1) + A_y(\alpha-1, \beta-1)]^2 + \left(\frac{\pi}{4a} \right)^2 [A_x(\alpha, \beta) + A_x(\alpha-1, \beta) + A_x(\alpha, \beta-1) + A_x(\alpha-1, \beta-1)]^2 + \left(\frac{\omega}{4c} \right)^2 [A_z(\alpha, \beta) + A_z(\alpha-1, \beta) + A_z(\alpha, \beta-1) + A_z(\alpha-1, \beta-1)]^2 - \left(\frac{1}{2\Delta y} \right)^2 [A_z(\alpha, \beta) - A_z(\alpha, \beta-1) + A_z(\alpha-1, \beta) - A_z(\alpha-1, \beta-1)]^2 - \left(\frac{1}{2\Delta x} \right)^2 [A_z(\alpha, \beta) - A_z(\alpha-1, \beta)]^2 \right\} \quad (3.14)$$

$$\begin{aligned}
& + A_z(\alpha, \beta-1) - A_z(\alpha-1, \beta-1)]^2 \\
& - \left[\frac{1}{2\Delta x} (A_y(\alpha, \beta) - A_y(\alpha-1, \beta) + A_y(\alpha, \beta-1) - A_y(\alpha-1, \beta-1)) \right. \\
& \left. - \frac{1}{2\Delta y} (A_x(\alpha, \beta) - A_x(\alpha, \beta-1) + A_x(\alpha-1, \beta) - A_x(\alpha-1, \beta-1)) \right]^2 \} .
\end{aligned}$$

We next wish to fix the field values at a small number of measurement points and vary all the fields not fixed by measurement or boundary condition until a stationary point is found. Because of our gauge choice and the fact that we are only considering a single frequency, a measurement of \bar{E} is a direct measurement of \bar{A} . The numerical calculation then proceeds as follows. The fields \bar{A} are fixed at measurement points, and the appropriate components are set equal to zero at the boundaries (eq (3.12)). These are not allowed to vary during the computation. A starting field configuration is generated according to the prescription

$$\begin{aligned}
A_x(x, y) &= \frac{B_x(y)}{R(\bar{x})} \sum_{n=1}^{N_m} A_x(X_n, Y_n) \frac{1}{|\bar{x} - \bar{x}_n|} \frac{1}{B_x(Y_n)} , \\
A_y(x, y) &= \frac{B_y(x)}{R(\bar{x})} \sum_{n=1}^{N_m} A_y(X_n, Y_n) \frac{1}{|\bar{x} - \bar{x}_n|} \frac{1}{B_y(X_n)} , \\
A_z(x, y) &= \frac{B_x(y) B_y(x)}{R(\bar{x})} \sum_{n=1}^{N_m} A_z(X_n, Y_n) \frac{1}{|\bar{x} - \bar{x}_n|} \frac{1}{B_x(Y_n) B_y(X_n)} ,
\end{aligned} \tag{3.15}$$

where R is just a normalization factor and the B functions enforce the boundary conditions,

$$\begin{aligned}
R(\bar{x}) &= \sum_{n=1}^{N_m} \frac{1}{|\bar{x} - \bar{x}_n|} , \\
B_x(y) &= (1 - e^{-2.3y/\xi})(1 - e^{-2.3(b-y)/\xi}) , \\
B_y(x) &= (1 - e^{-2.3x/\xi})(1 - e^{-2.3(a-x)/\xi}) ,
\end{aligned} \tag{3.16}$$

with ξ chosen to be $\lambda/4$. The vectors $\bar{X}_n = (X_n, Y_n)$ are the measurement points, and N_m is the number of measurements. The initial configuration given by eqs (3.15) and (3.16) is an arbitrary choice, but it does have the desirable properties that it smoothly interpolates between measurement points, obeys the boundary conditions, and is not the correct answer. The last point is important because the question is whether the computation can find the correct solution, not whether it recognizes the answer if given it.

Having generated initial values for all the $\bar{A}(i,j)$, we go through the grid setting the values of \bar{A} at each point (i,j) equal to the values required to make $\partial S/\partial A_a(i,j) = 0$ given the current values of \bar{A} at neighboring points. Such a procedure would drive us to a nearby extremum if only there were one. In either the continuous (3.11) or discrete (3.14) form, however, the action can be shown to have no (finite) extremum. The numerical procedure will then run away, given enough time. (This is true for any grid size; it just takes longer for finer grids.)

There is a way to locate the stationary point nevertheless. At a stationary point, S should change very little as we pass through the grid changing the $\bar{A}(i,j)$'s, and so we plot S as a function of the number of passes through the grid. Figure 3-4 shows the result for $a = 0.8\lambda$, $b = 0.4\lambda$. The program was told \bar{A} at nine points, (X_n, Y_n) with $X_n = a/4, a/2, 3a/4$, and $Y_n = b/4, b/2, 3b/2$. A 40×20 grid was used. The slope of the curve is quite small from $N \approx 40$ to $N \approx 90$; the approximate stationary point is somewhere in this range. The exact point doesn't matter much since the fields do not change much in this range of N . Figure 3-5 plots the fields as a function of x for a few values of y for $N = 65$. The correct solution is the TE_{10} mode, $A_x = A_z = 0$, $A_y(x,y) = \sin \frac{\pi x}{a}$ (solid line in figure). The crosses represent A_y , the circles A_x . The computed A_z is zero for all x and y and is not plotted. The results are clearly very good in this admittedly simple case, suggesting that the method holds some promise for practical applications.

We have also performed tests in which the number and positions of the measurement points were varied. Qualitatively, the results are about what one would expect. As fewer measurement points are taken, or when they are clumped together or all far from the center, the computed solution deteriorates. A worst case is only one measurement point (which only sets the scale of \bar{A}) far

from the center. For waveguide and grid as above, but with one measurement point at $(X_1, Y_1) = (0.1, 0.1)\lambda$, the action behaves as in figure 3-6. Again the general location of the approximate stationary point is apparent. Taking it to be at $N = 55$, one obtains the field configurations of figure 3-7. Although the agreement with the correct solutions is not so good as it was with nine measurements, it is still recognizable and would be quite useful if we only wanted an estimate of the maximum field within the enclosure.

This simple example may not have been a very demanding test, but the finite-element action approach did work; and it worked well enough to bolster our hope in the eventual practical applicability of the procedure.

3.4 Problems and Prospects

Although the waveguide example given above is a simple problem, the success of the finite-element action approach is significant nonetheless. The program did find a solution to a simple two-dimensional problem without knowing the source(s). Furthermore, many of the complexities of practical problems are little more than technical details in this approach. The extension to three spatial dimensions, for example, requires more computational time, but no new concepts or techniques. Also, because the symmetry of the waveguide has not been used, extension to irregular geometries should be no more difficult than specifying the geometry for the computer (provided the geometry is not such that it requires a hopelessly large number of grid points). Pieces of dielectric material can be included simply by storing the permittivity at each grid point, $\epsilon(i,j)$, and restoring $\epsilon(i,j)$ to eq (3.15).

The biggest unforeseen difficulty so far, that the stationary point is a saddle point, has been overcome. There are probably more elegant and/or efficient ways of finding the stationary point, but we have demonstrated that at least there is a way to find it. It is possible that the procedure can be modified so that the stationary point is a minimum, but we do not know how at this time, and it is not necessary as long as saddle points can be located.

All this is not to say that we are home free. It is possible that in practical problems the functional structure of S renders the stationary point much harder to locate. In addition, there are a number of technical hurdles

to be overcome before this technique becomes an everyday tool, but none of them is obviously insuperable. In a practical case boundary conditions could cause some trouble. Irregular boundaries are no problem in principle, but they will entail computational complications. A more serious difficulty is the handling of open boundary conditions. In the example given, the volume was completely enclosed, but one component was effectively free at each wall. When all three components are free over some part of the boundary surface, it is likely that some measured points will need to be on or near that surface to get good results. In the waveguide case we did try fixing the value of all components of \bar{A} on the boundary, and the only major effect was very close to the walls. This suggests that when open boundaries are present the buffer zone (cf. fig. 3-1), wherein we solve for the fields but do not believe the results, will not need to be too large.

There could also be difficulties associated with the measurements in practical problems. If more than one frequency is present, then a measurement of \bar{E} is not a direct measurement of \bar{A} , but rather of $\partial\bar{A}/\partial t$. Consequently not \bar{A} but rather its derivative must be held fixed in the computation. Similarly, a measurement of the magnetic field would fix a combination of derivatives of \bar{A} , not \bar{A} itself. Another difficulty is that it is much easier to measure the peak or average \bar{E} than it is to measure \bar{E} at one time t , but the latter quantity is the easier to include in the calculation. And, of course, eventually we need to confront the fact that the measurements are not perfect, and uncertainties must be included.

Other than the measurement complications just mentioned, complicated time dependence should not raise major difficulties. It increases the dimension of the problem--real problems will be four-dimensional as opposed to the two-dimensional example we did--but it is handled in much the same way as the spatial dimensions. It increases the computing time required, of course, but it requires no new developments.

As for the computation itself, no great effort has been made as yet to make it fast or efficient. For less simple geometries a different (e.g., triangular) gridding system would be more versatile, and the discretization of the integral (3.11-14) could also be improved. Such refinements and sophistications, however, fall in the fine-tuning category. The more immediate task

is to advance to more realistic problems and try to handle the concomitant complications. It appears that this action-based approach may be a viable practical method. If that proves to be the case we would have a very powerful method indeed; but considerable work, and perhaps even some ingenuity, is required before we reach that point.

4. Scanning Techniques

4.1 Cylindrical Scanning

The approach that is presented in this subsection involves cylindrical scanning. The ease with which a complex EM environment can be scanned by moving a highly directional probe along a single axis for different azimuthal orientations makes cylindrical scanning very attractive. The theoretical development given here is based on the source-scattering matrix [13], which is very analogous to the well-established plane-wave matrix approach [14].

A highly directional probe antenna and its coordinate system fixed to the probe antenna are shown schematically in figure 4-1. Unknown radiating sources are located outside a cylindrical volume, $\rho > \rho_0$. The EM fields in the source-free region ($\rho < \rho_0$) will be expanded in a complete set of cylindrical eigenfunctions,

$$\begin{aligned} \bar{E}(\rho, \phi, z) &= \sum_{n=-\infty}^{\infty} \int_{-\infty}^{\infty} [b_n^1(\gamma) \bar{M}_{n\gamma}(\rho, \phi, z) \\ &\quad + b_n^2(\gamma) \bar{N}_{n\gamma}(\rho, \phi, z)] d\gamma, \\ \bar{H}(\rho, \phi, z) &= \frac{j}{\omega\mu_0} \bar{\nabla}_x \bar{E} \\ &= \frac{j}{Z_0} \sum_{n=-\infty}^{\infty} \int_{-\infty}^{\infty} [b_n^1(\gamma) \bar{N}_{n\gamma}(\rho, \phi, z) + b_n^2(\gamma) \bar{M}_{n\gamma}(\rho, \phi, z)] d\gamma \end{aligned} \quad (4.1)$$

$$Z_0 = \sqrt{\mu_0/\epsilon_0} \approx 377 \Omega,$$

where the \bar{M} and \bar{N} functions are given by

$$\bar{M}_{n\gamma}(\rho, \phi, z) = \bar{\nabla}_x (J_n(K\rho) e^{-jn\phi} e^{-j\gamma z} \hat{e}_z)$$

$$= \left[\frac{-jn}{\rho} J_n(K\rho) \hat{e}_\rho - K J_n'(K\rho) \hat{e}_\phi \right] e^{-jn\phi} e^{-j\gamma z}$$

$$\bar{N}_{n\gamma}(\rho, \phi, z) = \frac{1}{k} \bar{\nabla} \times \bar{M}_{n\gamma} \quad (4.2)$$

$$= \frac{1}{k} \left[-j\gamma K J_n'(K\rho) \hat{e}_\rho - \frac{n\gamma}{\rho} J_n(K\rho) \hat{e}_\phi + K^2 J_n(K\rho) \hat{e}_z \right] e^{-jn\phi} e^{-j\gamma z}.$$

All quantities with a hat (^) over them denote unit vector; $e^{j\omega t}$ ($\omega > 0$) time dependence, and the rationalized mks systems are used throughout. The free-space wave number k is defined by $k = \omega \sqrt{\mu_0 \epsilon_0} = \frac{\omega}{c} = \frac{2\pi}{\lambda}$, the axial part of the wave propagation vector is denoted γ and $K = \sqrt{k^2 - \gamma^2}$. If one can use a probe antenna which measures the transverse (to \hat{e}_ρ) components of the electric field, then the $b_n(\gamma)$ can be determined directly. Namely, using the orthogonality relationship for the \bar{M} and \bar{N} functions, i.e.

$$\int_{-\infty}^{\infty} \int_0^{2\pi} (\bar{M}_{n\gamma} \times \bar{M}_{n'\gamma'}) \cdot \hat{e}_\rho \, d\phi \, dz = 0, \quad \int_{-\infty}^{\infty} \int_0^{2\pi} (\bar{N}_{nr} \times \bar{N}_{n'r'}) \cdot \hat{e}_\rho \, d\phi \, dz = 0 \quad (4.3)$$

$$\int_{-\infty}^{\infty} \int_0^{2\pi} (\bar{N}_{n\gamma} \times \bar{M}_{n'\gamma'}) \cdot \hat{e}_\rho \, d\phi \, dz = \frac{4\pi^2 k^3}{k} J_n(K\rho) J_n'(K\rho) \delta_{-n,n'} \delta(\gamma + \gamma').$$

By crossing \bar{N} into eq (4.1), one gets the $b_n^1(\gamma)$, i.e.

$$b_n^1(\gamma) = \frac{k}{4\pi k^3 J_{-n}^3(K\rho_0)} J_n'(K\rho_0) \int_{-\infty}^{\infty} \int_0^{2\pi} \{\bar{N} \times \bar{E}(\rho_0, \phi, z)\} \cdot \hat{e}_\rho \, d\phi \, dz \quad (4.4)$$

$$= \frac{-1}{4\pi^2 k^3 J_n^3(K\rho_0)} \int_{-\infty}^{\infty} \int_0^{2\pi} \left[\frac{n\gamma}{\rho_0} E_z(\rho_0, \phi, z) + K^2 E_\phi(\rho_0, \phi, z) \right] e^{jn\phi} e^{j\gamma z} \, d\phi \, dz.$$

Similarly, cross \bar{M} into (4.1) to yield the $b_n^2(\gamma)$,

$$b_n^2(\gamma) = \frac{k}{4\pi^2 k^2 J_n^2(K\rho_0)} \int_{-\infty}^{\infty} \int_0^{2\pi} E_z(\rho_0, \phi, z) e^{jn\phi} e^{j\gamma z} \, d\phi \, dz. \quad (4.5)$$

Equations (4.4,4.5) give the modal coefficients in terms of the measured transverse electric field. The efficient computation of the double integrals in eqs (4.4,4.5) can be carried out by use of the sampling theorem and a fast Fourier transform.

Consider a more general probe antenna whose receiving functions $R_n(\gamma)$ are known with respect to a cylindrical coordinate system fixed in the probe and centered on itself. The output of the probe is given by

$$b'_0 = \sum_{s=1}^2 \sum_{n=-\infty}^{\infty} \int_{-\infty}^{\infty} R_n^s(\gamma) a_n'^s(\gamma) d\gamma, \quad (4.6)$$

where $a_n'^s$ are the modal coefficients of the $J_n(K\rho)$ modes which are excited by sources existing outside the probe in the cylindrical coordinate (ρ', ϕ', z') system fixed in the source.

Specifically, the a_n^s field in cylindrical coordinates (ρ', ϕ', z') is given by

$$\bar{E}'(\rho', \phi', z') = \sum_{n=-\infty}^{\infty} \int_{-\infty}^{\infty} [a_n'^1(\gamma) \bar{M}_{n\gamma}^{(1)}(\rho', \phi', z') + a_n'^2(\gamma) \bar{N}_{n\gamma}^{(1)}(\rho', \phi', z')] d\gamma. \quad (4.7)$$

$$\bar{H}'(\rho', \phi', z') = \frac{1}{jZ_0} \sum_{n=-\infty}^{\infty} \int_{-\infty}^{\infty} [b_n'^1(\gamma) \bar{N}_{n\gamma}^{(1)}(\rho', \phi', z') + b_n'^2(\gamma) \bar{M}_{n\gamma}^{(1)}(\rho', \phi', z')] d\gamma$$

Now $\bar{M}_{n\gamma}$ is defined as before.

$$\begin{aligned} \bar{M}_{n\gamma}^{(1)}(\rho, \phi, z) &= \bar{\nabla} \times J_n(K\rho) e^{-jn\phi} e^{-j\gamma z} \hat{e}_z \\ &= \left[-\frac{jn}{\rho} J_n(K\rho) - K J_n'(K\rho) \right] e^{-jn\phi} e^{-j\gamma z} \hat{e}_\phi \end{aligned} \quad (4.8)$$

$$\begin{aligned} \bar{N}_{n\gamma}^{(1)}(\rho, \phi, z) &= \frac{1}{K} \bar{\nabla} \times \bar{M}_{n\gamma}^{(1)} \\ &= \frac{1}{K} \left[-j\gamma K J_n'(K\rho) \hat{e}_\rho - \frac{n\gamma}{\rho} J_n(K\rho) \hat{e}_\phi + K^2 J_n(K\rho) \hat{e}_z \right] e^{-jn\phi} e^{-j\gamma z}. \end{aligned}$$

Now, regardless of whether the probe antenna or EM source coordinate system is used, the EM field at every point in space must be the same.

$$\bar{E}'(\rho', \phi', z') = \bar{E}(\rho, \phi, z) \quad (4.9)$$

$$\bar{H}'(\rho', \phi', z') = \bar{H}(\rho, \phi, z)$$

when (ρ', ϕ', z') and (ρ, ϕ, z) refer to the same point in space. But as the probe antenna scans the radiation source, the source coordinate system is merely rotated through an angle ϕ_0 , about the z-axis, and translated a distance z_0 along the z-axis, i.e.

$$\rho' = \rho, \phi' = \phi - \phi_0 \text{ and } z' = z - z_0 \quad (4.10)$$

and eq (4.9) becomes

$$\begin{aligned} \bar{E}'(\rho, \phi - \phi_0, z - z_0) &= \bar{E}(\rho, \phi, z) \\ \bar{H}'(\rho, \phi - \phi_0, z - z_0) &= \bar{H}(\rho, \phi, z) \end{aligned} \quad (4.11)$$

when (\bar{E}, \bar{H}) and (\bar{E}', \bar{H}') are written explicitly in terms of the linearly independent cylindrical waves in eqs (4.1) and (4.7). The orthogonality relations eq (4.3) show that the only way eq (4.11) can be satisfied is if

$$a_n^{iS}(\gamma) = b_n^S(\gamma) e^{-jn\phi_0 - jnz_0}, \quad s=1,2. \quad (4.12)$$

Thus the probe receiving equation becomes

$$b'(\phi_0, z_0) = \sum_{s=1}^2 \sum_{n=-\infty}^{\infty} \int_{-\infty}^{\infty} R_n^S(\gamma) b_n^S(\gamma) e^{-jn\phi_0 - jz_0} d\gamma. \quad (4.13)$$

Let us discuss how to evaluate some characteristics of $b_n^S(\gamma)$. In principle, as the probe antenna scans the EM environment, the output $b'(\phi_0, z_0)$ of the probe antenna is recorded for

$$0 < \phi_0 < 2\pi \text{ and } -\infty < z_0 < \infty.$$

That is, the amplitude and phase of $b'(\phi_0, z_0)$ are measured for all values of ϕ_0 and z_0 . In practice, the z_0 scan can be limited to some finite scan length, since $b'_0(\phi_0, z_0)$ is assumed negligible outside this region. Also, data need be sampled and recorded only at a finite number of measurement points. Having measured $b'(\phi_0, z_0)$, the Fourier series and integral of eq (4.13) can be immediately inverted to yield the solution

$$\sum_{S=1} R_n^S(\gamma) b_n^S(\gamma) = [R_n^1(\gamma) b_n^1(\gamma) + R_n^2(\gamma) b_n^2(\gamma)]$$

$$= \frac{1}{4\pi^2} \int_{-\infty}^{\infty} \int_0^{2\pi} b_0'(\phi_0, z_0) e^{jn\phi_0} e^{j\gamma z_0} d\phi_0 dz_0 \equiv I_n(\gamma) \quad (4.14)$$

Since eq (4.14) involves two unknowns $b_n^1(\gamma)$ and $b_n^2(\gamma)$, two linearly independent scans are necessary to account for the polarization of the EM fields. The second scan produces a second equation to complement eq (4.14), i.e.,

$$\sum_{S=1}^2 R_n^{iS}(\gamma) b_n^S(\gamma) = R_n^{i1}(\gamma) b_n^1(\gamma) + R_n^{i2}(\gamma) b_n^2(\gamma) \quad (4.15)$$

$$= \frac{1}{4\pi^2} \int_{-\infty}^{\infty} \int_0^{2\pi} b_0'(\phi_0, z_0) e^{jn\phi_0} e^{j\gamma z_0} d\phi_0 dz_0 \equiv I_n^i(\gamma)$$

where $R_n^{iS}(\gamma)$ and $b_0'(\phi_0, z_0)$ are the receiving characteristic and the output of reoriented probe, respectively.

Assuming for the moment that the receiving function (R^{i1}, R^{i2}) of the probe antenna is known, eqs (4.14) and (4.15) can be solved immediately for the source characteristic $b(\gamma)$, i.e.

$$b^1(\gamma) = [R_n^{i2}(\gamma) I_n(\gamma) - R_n^2(\gamma) I_n^i(\gamma)] / \Delta_n(\gamma) \quad (4.16)$$

$$b^2(\gamma) = [R_n^{i1}(\gamma) I_n^i(\gamma) - R_n^1(\gamma) I_n(\gamma)] / \Delta_n(\gamma)$$

where

$$\Delta_n(\gamma) = R_n^{i2}(\gamma) R_n^1(\gamma) - R_n^2(\gamma) R_n^{i1}(\gamma) \quad (4.17)$$

Equation (4.16) indicates that the cylindrical wave expansion coefficients b_n^1 and b_n^2 for the EM complex field environment can be determined provided the receiving characteristics of the probe antenna are known. There are several ways to determine the receiving characteristics of a general probe antenna in terms of the scalar cylindrical waves. Since it is beyond the scope of this paper, it will be discussed in a future paper. But it is very easy to show that, if a probe antenna is an ideal electric dipole, i.e., a probe that measures the transverse components of the electric field, then eqs (4.4) and (4.5) emerge immediately from (4.16) and (4.17). For more directional probes,

a different expansion may be more useful, and we next turn our attention to this possibility.

4.2 Spherical (Directional) Scanning

If one has a probe which is highly directional, this feature can be used for directional or spherical scanning at one point, a suggestion due to Chang and Maley [15]. The directional features are most directly exploited by a plane-wave expansion. Assuming a single frequency, the electric field is written as

$$\begin{aligned}\bar{E}(\bar{x}, t) &= \bar{E}(\bar{x}) e^{j\omega t}, \\ \bar{E}(\bar{x}) &= \int \frac{d^3k}{(2\pi)^3} e^{-j\bar{k} \cdot \bar{x}} \bar{E}(\bar{k}).\end{aligned}\tag{4.18}$$

If \bar{E} is to satisfy Maxwell's equations, we must have $k^2 = \omega^2/c^2$, allowing us to write (for large volumes)

$$\begin{aligned}\bar{E}(\bar{k}) &= \bar{e}_k(\hat{k}) 2\pi\delta\left(\frac{\omega}{c} - k\right), \\ \bar{E}(\bar{x}) &= \frac{k^2}{(2\pi)^2} \int d\Omega_k e^{-j\bar{k} \cdot \bar{x}} \bar{e}_k(\theta, \phi).\end{aligned}\tag{4.19}$$

It is necessary at this point to set forth the notational conventions for this subsection since many different angles will be encountered. There are two coordinate systems of interest, one fixed with respect to the volume of interest (the "lab" coordinate system), and one fixed with respect to the probe (the "probe" coordinate system), cf. figure 4-2. The two coordinate systems have a common origin, the location of the probe (assumed to be small). The ζ axis of the probe system is described by angles θ_0, ϕ_0 in the lab system; the ξ axis of the probe system is chosen to lie in the $\hat{z} \times \hat{\zeta}$ plane. In the course of the scanning θ_0 and ϕ_0 vary, of course. The direction of incidence of a plane wave with respect to the probe system will be denoted θ', ϕ' . This same direction as seen in the lab system is called θ, ϕ . The angles θ, ϕ depend not only on θ', ϕ' but also on θ_0, ϕ_0 . And conversely $\theta' = \theta'(\theta, \phi, \theta_0, \phi_0)$, $\phi' = \phi'(\theta, \phi, \theta_0, \phi_0)$. A straightforward exercise

with rotation matrices yields the relations

$$\cos \theta' = \sin \theta_0 \sin \theta \cos(\phi - \phi_0) + \cos \theta_0 \cos \theta, \quad (4.20)$$

$$\cot \phi' = \cot(\phi - \phi_0) \cos \theta_0 - \sin \theta_0 \cot \theta \csc(\phi - \phi_0).$$

For the sake of simplicity and clarity in this presentation, we limit ourselves to the case of a scalar field. The response of the probe to a single plane wave incident at angles θ', ϕ' in the probe coordinate system will be the product of the probe acceptance at that angle (A), the amplitude per solid angle of the wave (e'_k), and the solid angle,

$$dR = A(\theta', \phi') e'_k(\theta', \phi') d\Omega'. \quad (4.21)$$

But the plane wave component from θ', ϕ' in the probe system is the same as the component from $\theta(\theta', \phi', \theta_0, \phi_0), \phi(\theta', \phi', \theta_0, \phi_0)$ in the lab system,

$$e'_k(\theta', \phi') = e_k(\theta(\theta', \phi', \theta_0, \phi_0), \phi(\theta', \phi', \theta_0, \phi_0)). \quad (4.22)$$

Using this fact and integrating the differential response (4.21) over all incident angles in the probe system, we obtain for the total response

$$R(\theta_0, \phi_0) = \int_{-1}^1 d \cos \theta' \int_{-\pi}^{\pi} d\phi' A(\theta', \phi') e_k(\theta(\theta', \phi', \theta_0, \phi_0), \phi(\theta', \phi', \theta_0, \phi_0)). \quad (4.23)$$

For purposes of numerical inversion, we find it more convenient to rewrite eq (4.23) as an integration over lab-system angles,

$$R(\theta_0, \phi_0) = \int_{-1}^1 d \cos \theta \int_{-\pi}^{\pi} d\phi A(\theta(\theta, \phi, \theta_0, \phi_0), \phi(\theta, \phi, \theta_0, \phi_0)) e_k(\theta, \phi). \quad (4.24)$$

If the probe is perfectly directional A is just a product of delta functions of $\theta - \theta_0$ and $\phi - \phi_0$; and the response at θ_0, ϕ_0 measures $e_k(\theta_0, \phi_0)$ directly. For imperfect directional probes, a little more work is required. The probe response is recorded for some number N_{meas} of scan angles

$\theta_i, \phi_i, i = 1, N_{\text{meas}}$. We must invert (4.24) to obtain $e_k(\theta, \phi)$, which then determines the field throughout the volume from eq (4.19).

To invert eq (4.24) we use a pulse expansion of $e_k(\cos \theta, \phi)$ and point matching. Assume for simplicity that the scanning was done at regular intervals δ_θ in $\cos \theta$ and δ_ϕ in ϕ . Let

$$e_k(\theta, \phi) \approx \sum_{n=1}^{N_\theta} \sum_{m=1}^{N_\phi} e_k^{nm} \Pi_{nm}(\cos \theta, \phi), \quad (4.25)$$

$$N_\theta = 2/\delta_\theta, \quad N_\phi = 2\pi/\delta_\phi,$$

where $\Pi_{nm}(\cos \theta, \phi)$ is the unit pulse function centered at $\cos \theta = -1 + (n - \frac{1}{2})\delta_\theta$, $\phi = (m - \frac{1}{2})\delta_\phi$,

$$\begin{aligned} \Pi_{nm}(\cos \theta, \phi) &= 1 & -1 + (n - 1)\delta_\theta < \cos \theta < -1 + n\delta_\theta \\ & & \text{and } (m-1)\delta_\phi < \phi < m\delta_\phi, \\ &= 0 & \text{otherwise.} \end{aligned} \quad (4.26)$$

For each of the N_{meas} measurement directions we get an equation of the form

$$R(\theta_i, \phi_i) \approx \sum_{n=1}^{N_\theta} \sum_{m=1}^{N_\phi} e_k^{nm} A^{nm}(\theta_i, \phi_i), \quad (4.27)$$

$$A^{nm}(\theta_i, \phi_i) \equiv \int_{-1+(n-1)\delta_\theta}^{-1+n\delta_\theta} d \cos \theta \int_{(m-1)\delta_\phi}^{m\delta_\phi} d\phi A(\theta'(\theta, \phi, \theta_i, \phi_i), \phi'(\theta, \phi, \theta_i, \phi_i)).$$

Because the measurement angles coincide with the centers of the pulses, it is a simple matter to relabel indices and force eq (4.27) into the form of a simple matrix equation. The m and n indices are combined into one index running from 1 to $N_{\text{meas}} = N_\theta \times N_\phi$,

$$\begin{aligned} g_k^1 &\equiv e_k^{11}, \quad g_k^2 \equiv e_k^{12}, \quad \dots, \quad g_k^{N_\phi+1} = e_k^{21}, \quad \dots, \\ a_i^1 &\equiv A^{11}(\theta_i, \phi_i), \quad a_i^2 \equiv A^{12}(\theta_i, \phi_i), \quad \dots, \end{aligned} \quad (4.28)$$

$$R_i \equiv R(\theta_i, \phi_i).$$

Then eq (4.27) takes the form

$$R_i = \sum_{\ell=1}^{N_{\text{meas}}} a_i^\ell g_k^\ell, \quad (4.29)$$

$$g_k^j = \sum_i (a^{-1})^{ji} R_i.$$

The e_k^{nm} 's are then substituted into eq (4.25) to yield the approximation for $e_k(\theta, \phi)$, which in turn is substituted into eq (4.19) to yield the field $E(\bar{x})$.

We thus can obtain an estimation of $E(\bar{x})$ even with only a few scanning angles, though of course the approximation becomes better as more measurements are made. It remains to be seen how large the angular increments in the scanning can be in practical applications. The expansion of eq (4.19) will only be valid for $|\bar{x}|$ less than the distance to the first source or scatterer, but the method still offers the promise of an estimate of the field throughout a volume, from a limited number of measurements at just one point.

5. Summary

As more sources contribute to ambient electromagnetic fields, and as the electronic devices operating in these ambient fields become more numerous, sensitive, and important, the problem of efficiently measuring and characterizing complicated electromagnetic environments is becoming increasingly acute. We have discussed three different approaches to the problem, outlining the foundation, present status, and direction of future development of each. Because there is so little previous work on characterization of complicated electromagnetic environments, any new method tends to require completely new development beginning from the basics, and as a result progress can be rather slow.

Each method discussed is quite promising in the sense that each appears to have a reasonable chance of actually working, and each will be very useful if it does work. However, each method also requires further development and work. That work is in progress.

6. References

- [1] Kanda, M. Time and amplitude statistics for electromagnetic noise in mines, IEEE Trans. on Electromagnetic Compatibility. Vol. EMC-17, No. 3: 122-129, August 1975.
- [2] Beckmann, P. Probability in communication engineering. New York, NY: Harcourt, Brace and World, Inc.; 1967.
- [3] Lee, W.C.Y. Mobile communications engineering. New York, NY: McGraw-Hill Book Company; 1982.
- [4] Wells, P. I.; Hill, D. A.; Longley, A. G.; FitzGerrell, R. G.; Haidle, L. L. and Glen, D. V. An experiment design for the measurement of building attenuation, OT Technical Memorandum 75-199, May 1975.
- [5] Hoffman, H. H.; Cox, D. C. Attenuation of 900 MHz radio waves propagating into a metal building, IEEE Trans. on Antennas and Propagation, Vol. AP-30, No. 4, 808-811, July 1982.
- [6] Cox, D. C.; Murray, R. R.; Norris, A. W. Measurements of 800 MHz radio transmission into buildings with metallic walls. The Bell System Technical Journal, Vol. 62, No. 9, 2695-2717; November 1984.
- [7] Ishimaru, A.; Sigelmann, R. A.; Kuza, Y. Private communication.
- [8] Landau, L. D.; Lifshitz, E. M. The classical theory of fields, Chapter 4, Reading, MA: Addison-Wesley, 1962.
Morse, P. M.; Feshbach, H. Methods of theoretical physics, Chapter 3, New York, NY: McGraw-Hill, 1953.
- [9] Whittaker, E. T. Treatise on the analytical dynamics of particles and rigid bodies, Chapter 9, New York, NY: Dover, 1944.
- [10] Ferrari, R. L.; Maile, G. L. Three-dimensional finite-element method for solving electromagnetic problems, Electron. Lett. Vol. 14, No. 15, 467-468; 1978.

- Webb, J. P.; Maile, G. L.; Ferrari, R. L. Finite-element solution of three-dimensional electromagnetic problems, IEE Proc. Vol. 130H, No. 2, 153-159; 1983.
- Rahman, B. M. A.; Davies, J. B. Finite-element analysis of optical and microwave waveguide problems, IEEE Trans. on MTT, Vol. MTT-32, No. 1, 20-28; 1984.
- [11] Morishita, K.; Kumagai, N. Unified approach to the derivation of variational expression for electromagnetic fields, IEEE Trans. on MTT, Vol. MTT-25, No. 1, 34-40; 1977.
- [12] Ramond, P. Field theory: A modern primer, Reading, MA: Benjamin/Cummings, 1981.
- Itzykson, C.; Zuber, J. B. Quantum field theory, New York, NY: McGraw-Hill, 1980.
- [13] Yaghjian, A. D. Near-field antenna measurements on a cylindrical surface: A source scattering-matrix formulation. Nat. Bur. Stand. (U.S.) Tech. Note 696; 1977 September.
- [14] Kerns, D. M. Plane-wave scattering-matrix theory of antennas and antenna-antenna interactions: formulation and applications. J. Res. Nat. Bur. Stand. (U.S.). 80B: 1, 5-51; 1976 January-March.
- Kerns, D.M. Plane-wave scattering-matrix theory of antennas and antenna-antenna interactions. Nat. Bur. Stand. (U.S.). Monogr. 162, 179 p., June 1981.
- [15] Chang, D. C. and Maley, S. Private communication.

Appendix

In order to locate a stationary point of the action we need to know whether we are looking for a maximum, a minimum, or neither. In addition, if it is an extremum, we would like to know whether it is a global or only a local extremum. It is often assumed that it is a minimum, but our experience indicates that exceptions are neither so rare nor so pathological as one might expect.

For mechanical systems the problem is addressed in Whittaker's classic treatise [9]. (Note that Whittaker uses the word "action" for a different quantity than we do. It is, however, a difference of nomenclature not substance.) The type of stationary point which S has depends on the "kinetic focus" of the original point, defined as follows. Consider a point A on an actual trajectory; and let another actual trajectory pass through A , at some small angle with respect to the first. If the two trajectories intersect again, say at point B , then the kinetic focus of A is the limiting value of B as the angle between the two trajectories at A goes to zero. The relevant result then is that the stationary point of the action S is a minimum if the final point in the integration occurs before the kinetic focus of the initial point; if it occurs after the kinetic focus the stationary point is neither a minimum nor maximum but rather a saddle point.

To make sense of the preceding verbiage, an example is in order. Whittaker considers a particle on a sphere with no forces acting. For variety, and because it is a little more relevant for us, we consider a simple harmonic oscillator such as a mass (m) on a spring (spring constant k). The action is

$$S = \frac{m}{2} \int_{t_i}^{t_f} dt [\dot{x}(t)^2 - \frac{k}{m} x(t)^2], \quad (\text{A.1})$$

where $x(t)$ is the position at time t . The kinetic focus for a given $x_i = x(t_i)$ is easily determined from our knowledge of the solutions. Since solutions of different amplitude all have the same period, if two trajectories (solutions) are both at x_i at time t_i , then one half period later both will be at $x = -x_i$. Consequently, the kinetic focus of t_i occurs at $t = t_i + T/2 = t_i + \pi\sqrt{m/k}$. We therefore expect the stationary point of S will be a minimum for $t_f < t_i + T/2$ and a saddle point if $t_f > t_i + T/2$.

We can verify this expectation by direct calculation. If we vary $x(t)$ and set the first variation of S equal to zero we just obtain the equation of motion. Considering the second order variation of S , we have

$$\frac{2}{m} \delta_x^2 S = \int_{t_i}^{t_f} dt [(\delta\dot{x})^2 - \frac{k}{m} (\delta x)^2] \quad (\text{A.2})$$

$$= \left[\delta x \dot{\delta x} \right]_{t_i}^{t_f} - \int_{t_i}^{t_f} dt \delta x \left[\dot{\delta x} + \frac{k}{m} \delta x \right].$$

The first term vanishes because $\delta x(t) = 0$ at the end points $t = t_i, t_f$. This fact also allows us to expand $\delta x(t)$ in a discrete Fourier sine series,

$$\delta x(t) = \sum_{n=1}^{\infty} \delta x_n \sin [n \pi (t-t_i)/\Delta t], \quad (A.3)$$

$$\Delta t \equiv t_f - t_i.$$

Substituting eq (A.3) in eq (A.2) yields

$$\frac{2}{m} \delta^2 S = \frac{\Delta t}{2} \sum_{n=1}^{\infty} \left[\left(\frac{n\pi}{\Delta t} \right)^2 - \frac{k}{m} \right] \delta x_n^2. \quad (A.4)$$

Since the original $\delta x(t)$ was arbitrary, so too are all the δx_n 's. Therefore, $\delta^2 S$ will always be positive only if $[(n\pi/\Delta t)^2 - k/m] > 0$ for all n . This requires

$$\Delta t < \pi \sqrt{\frac{m}{k}} = \frac{1}{2} T. \quad (A.5)$$

For $\Delta t > T/2$, $\delta^2 S$ can be positive or negative depending on the choice of $\delta x(t)$. Therefore, as expected, the stationary point is a minimum if t_f is earlier than the kinetic focus, and a saddle point if t_f is after the kinetic focus. (If t_f occurs at the kinetic focus, $\delta^2 S > 0$.)

Transferring these results to the electromagnetic problems of interest requires further work; but there are reasons, both heuristic and empirical, for expecting the stationary point to be a saddle point. One heuristic reason is that we are formally considering $\int dt L$, so that t_f must be later than the kinetic focus provided it exists. Secondly, in the mechanical case the transition from minimum to saddle point is related to the nonuniqueness of the solution. For the harmonic oscillator example, for $t_f < t_i + T/2$ specifying $t_i, t_f, x(t_i)$, and $x(t_f)$ specifies a unique solution (i.e. amplitude and phase). However, for $t_f = t_i + T/2$ there is a continuum of solutions possible for a given $t_i, t_f, x(t_i), x(t_f)$. This is no coincidence since the kinetic focus occurs at the (limit of the) intersection of real trajectories passing through the initial point. It is then reasonable to infer that the stationary

point ceases to be a minimum when t_f exceeds the first time at which it is possible to have more than one solution. The nonuniqueness of the solutions in the electromagnetic problems we are attacking was noted earlier, and so we have another qualitative reason to expect a saddle point.

Finally, there is the empirical evidence: in the example problem presented in subsection (3.3), the stationary point is shown to be a saddle point. This is a potential disaster computationally, but it will prove possible to locate the saddle point.

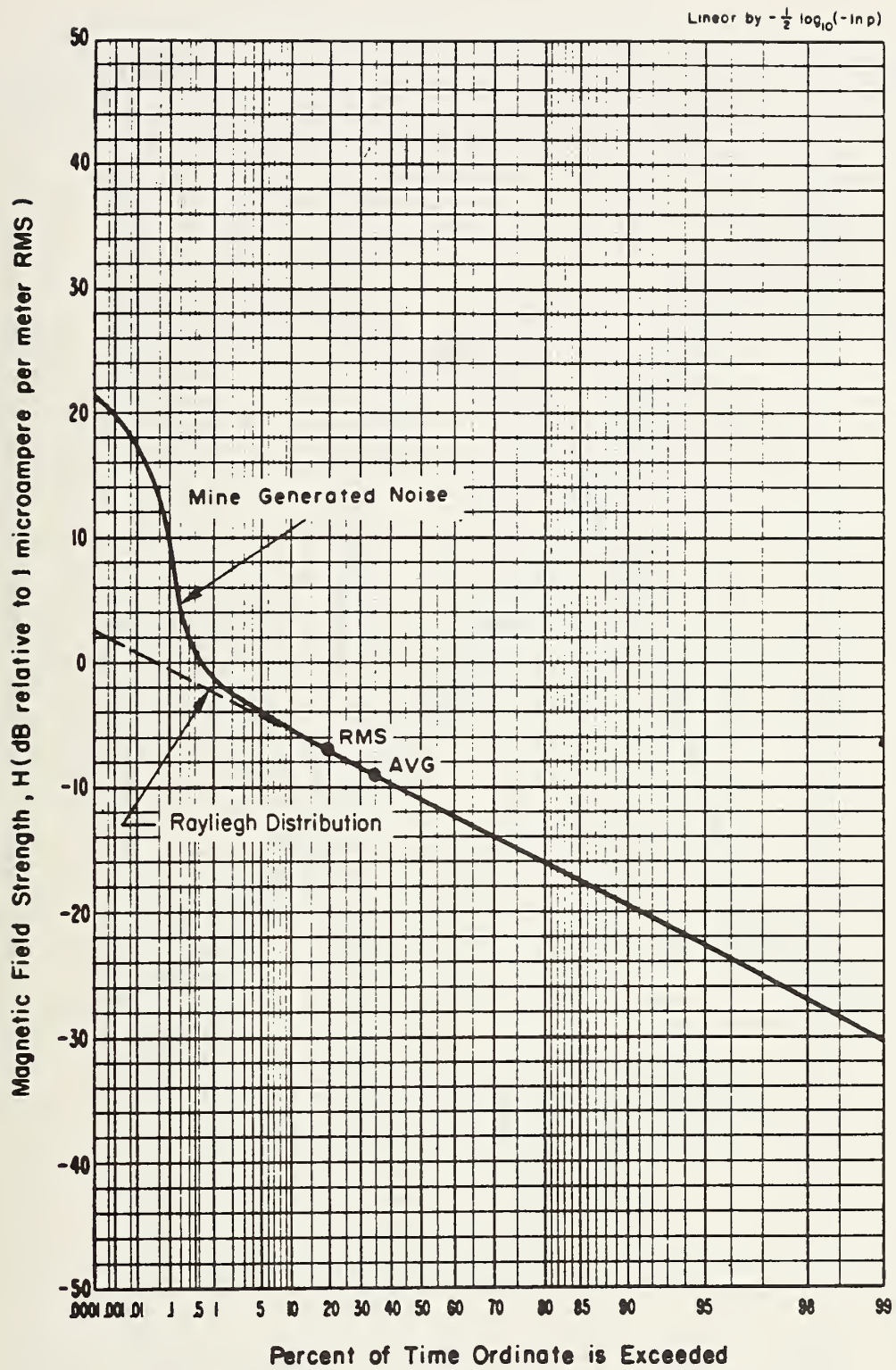


Figure 2-1. Cumulation amplitude probability distribution of EM noise in a mine.

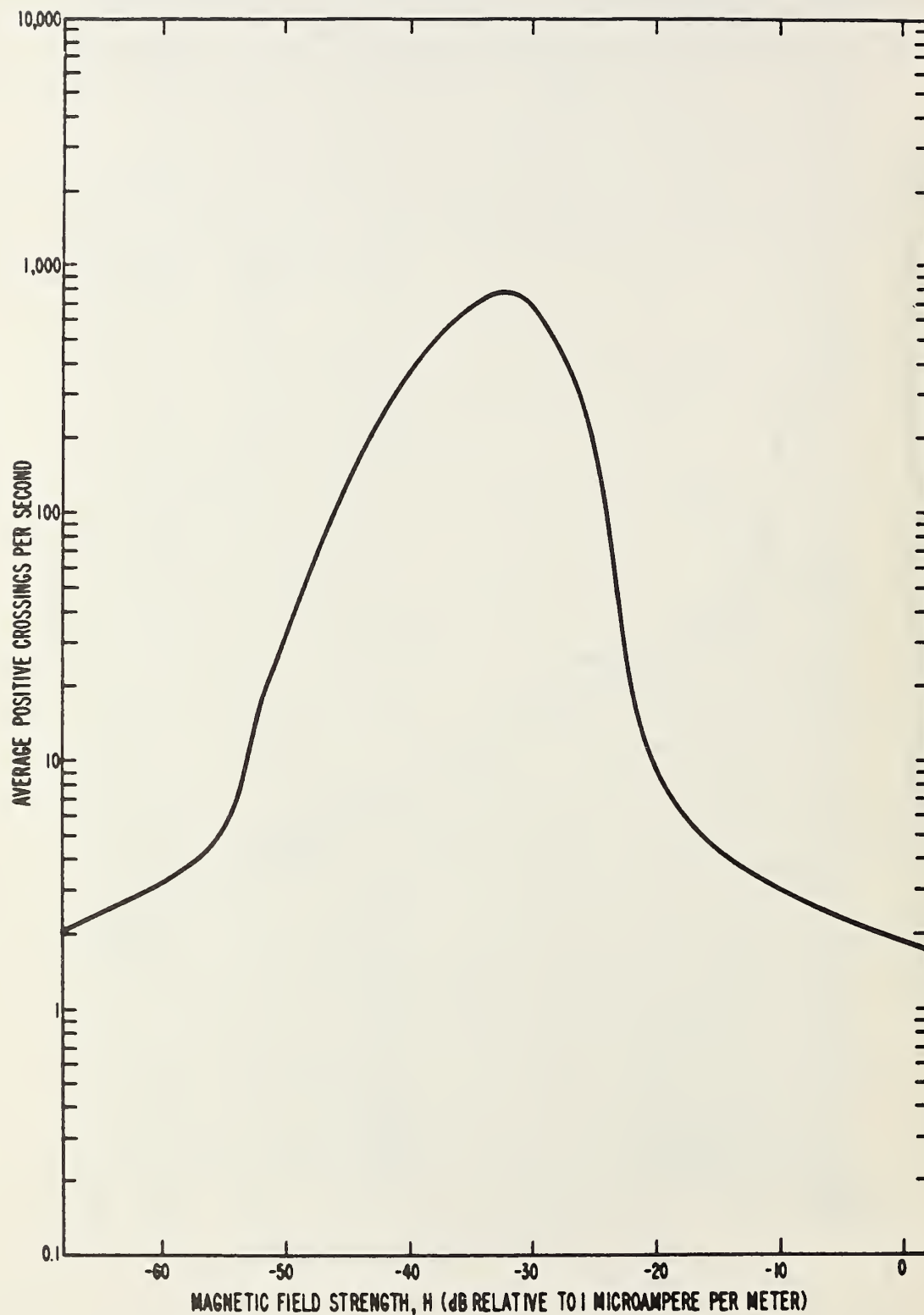


Figure 2-2. Average crossing rate of EM noise in a mine.

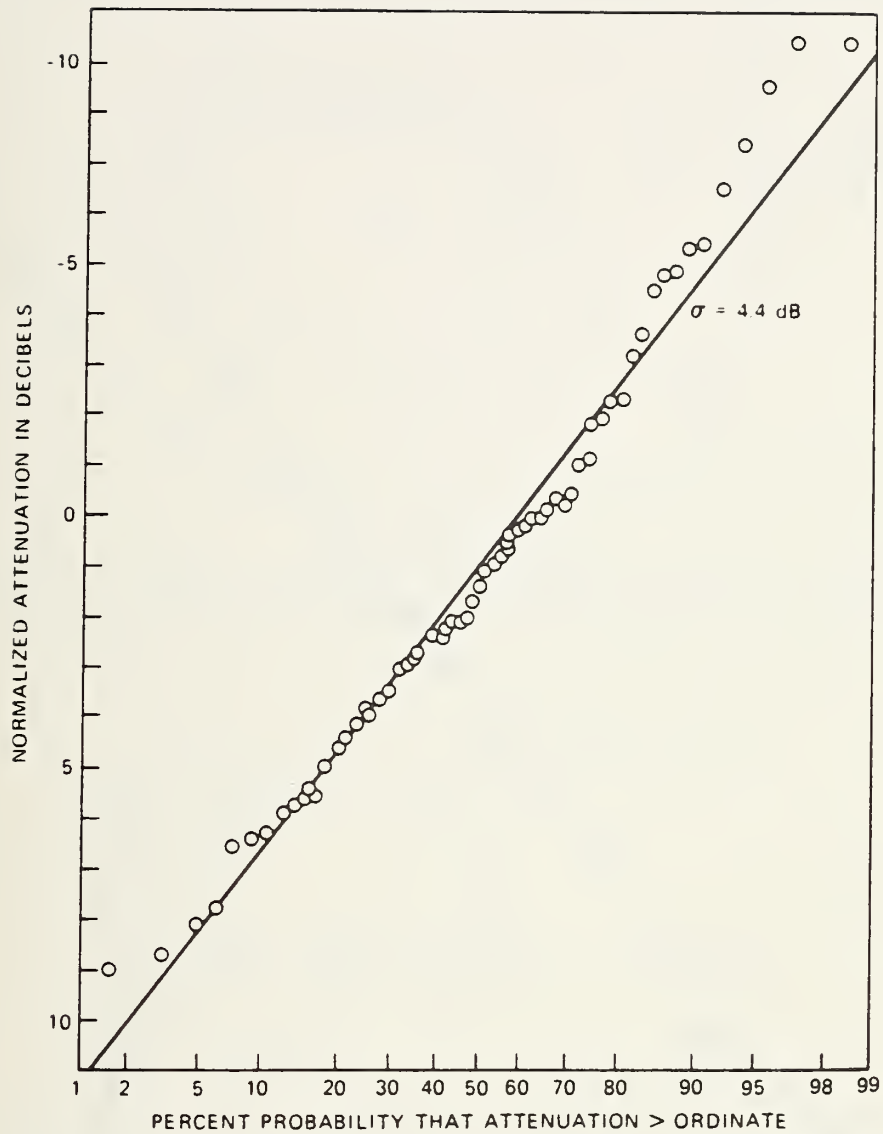


Figure 2-3. Cumulative amplitude probability distribution of the building's attenuations. [6] The straight line represents a log-normal distribution.

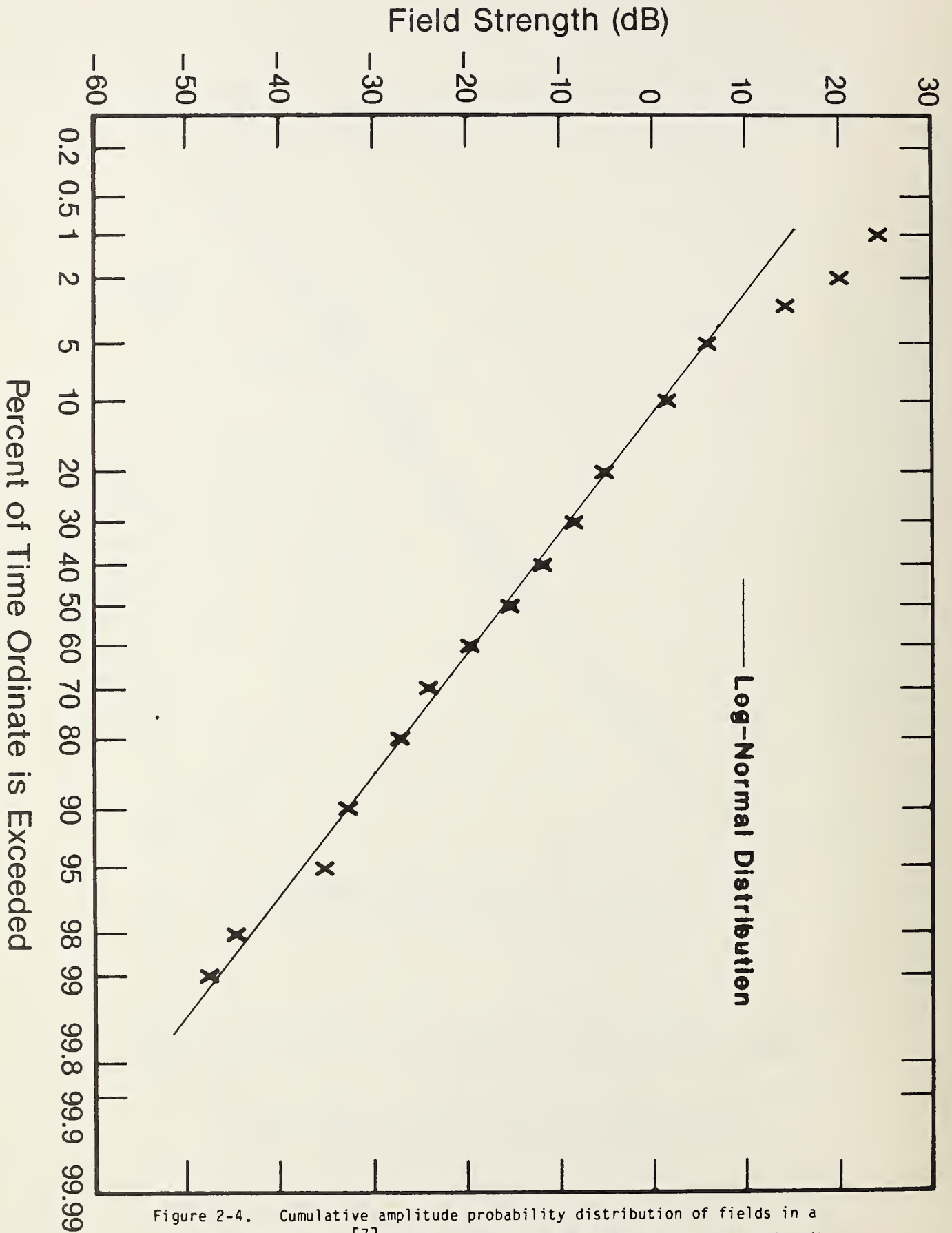


Figure 2-4. Cumulative amplitude probability distribution of fields in a rectangular cavity.^[7] The straight line represents a lognormal distribution.

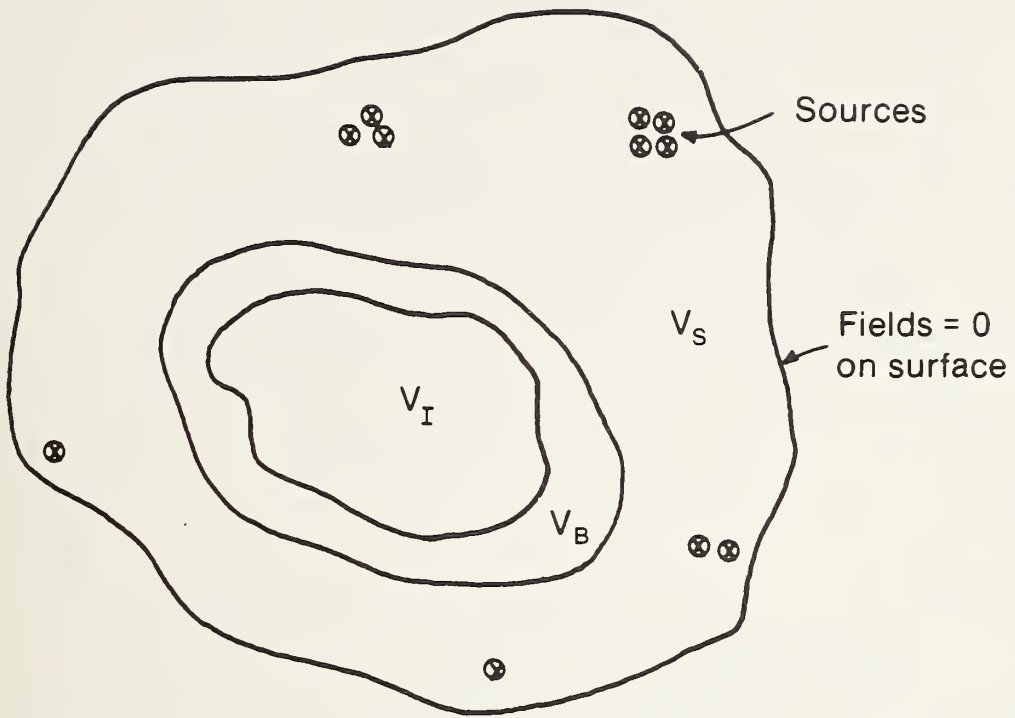


Figure 3-1. Schematic division of total volume into volume of interest (V_I), buffer volume (V_B), and remaining volume containing all sources (V_S).

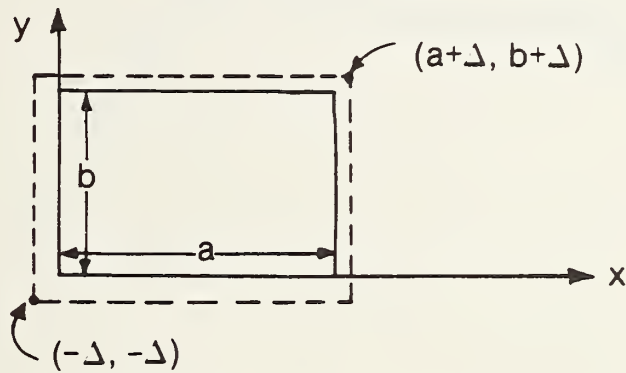


Figure 3-2. Rectangular waveguide dimensions and axes. Also depicted is the boundary of the volume over which the action integral extends.

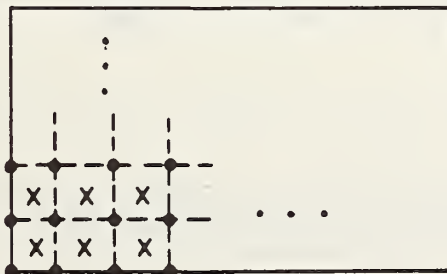


Figure 3-3. Lattice of points for finite-element action.

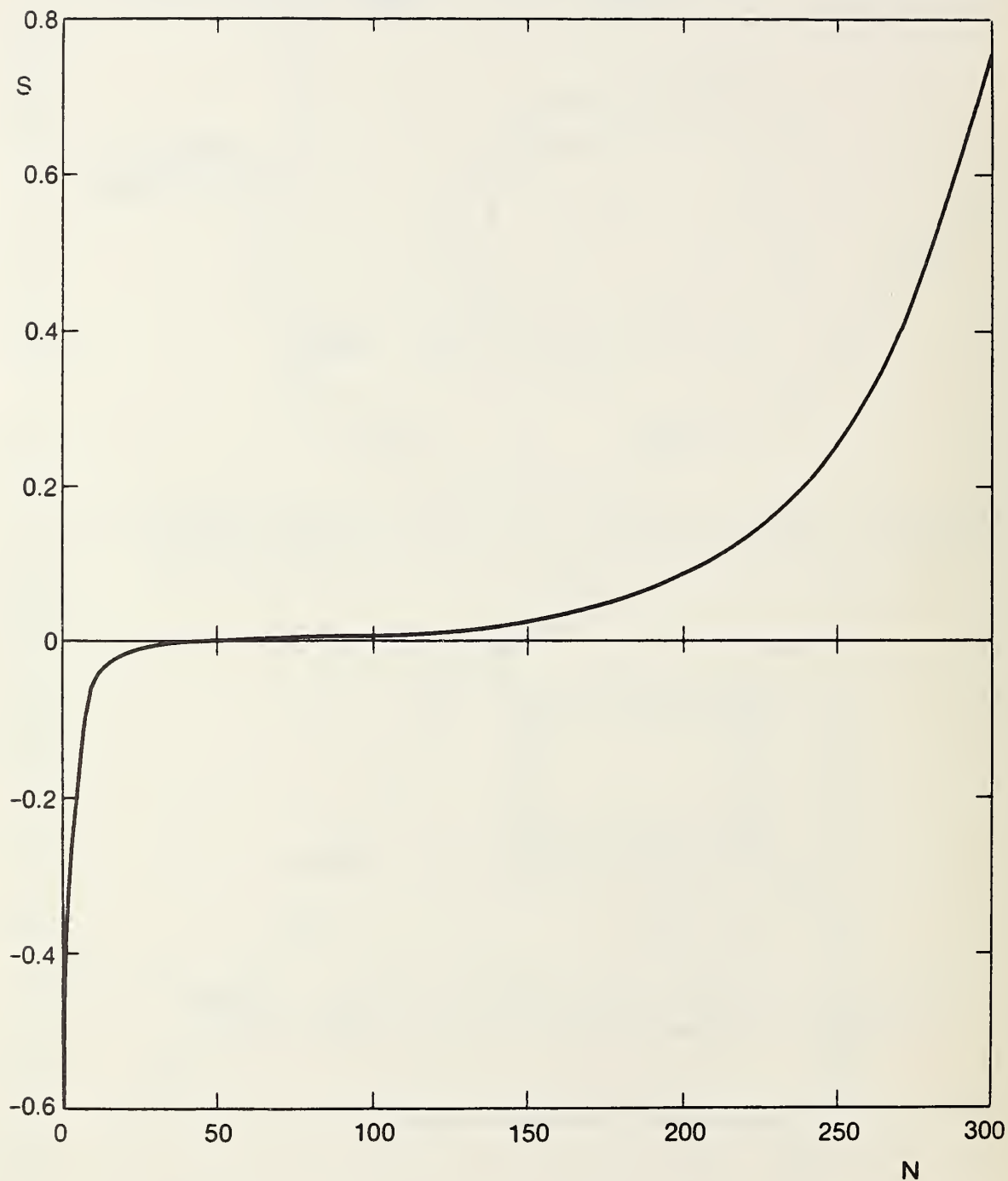


Figure 3-4. Action as a function of N, the number of passes through the grid in the numerical computation, for nine measurement points.

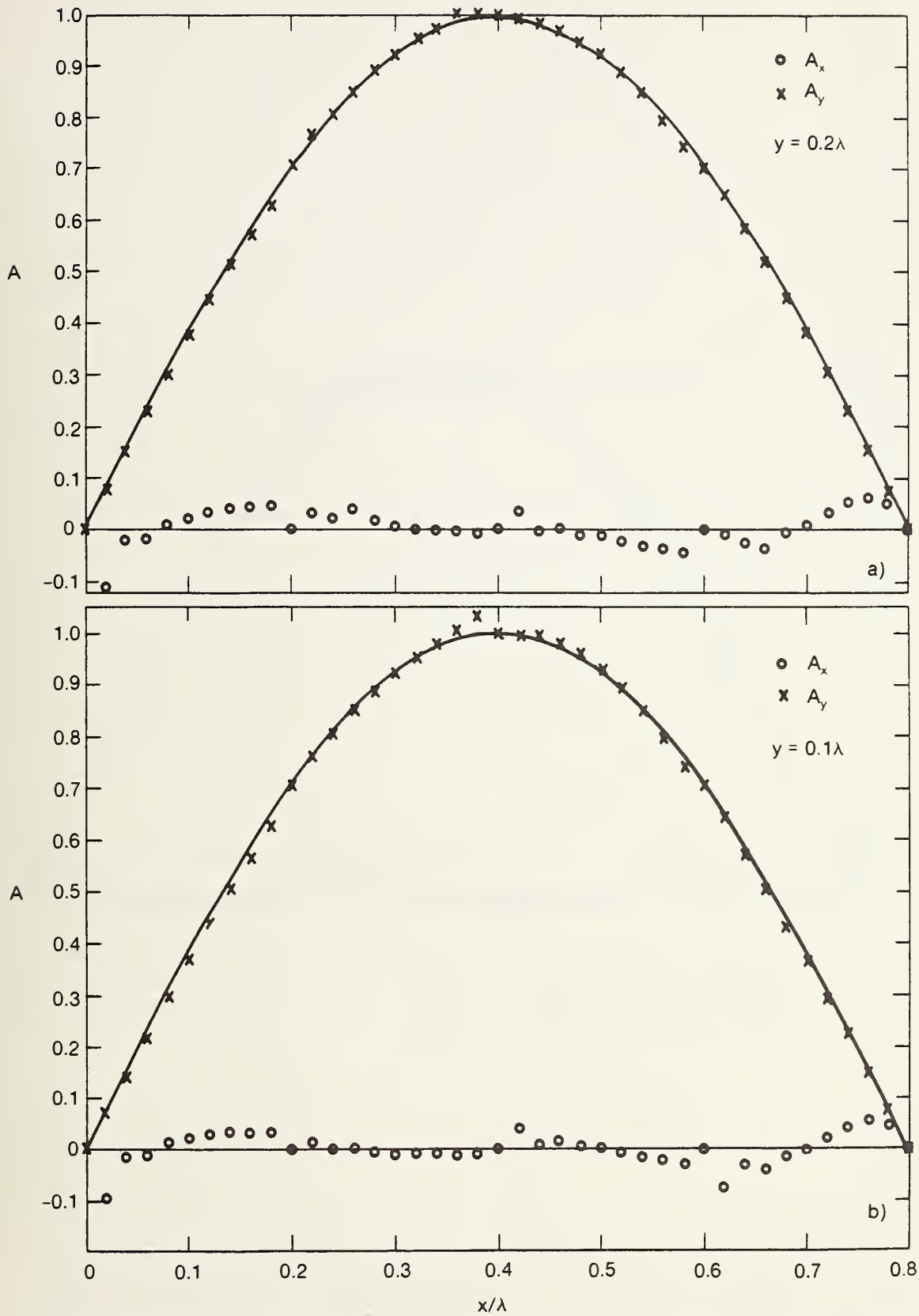
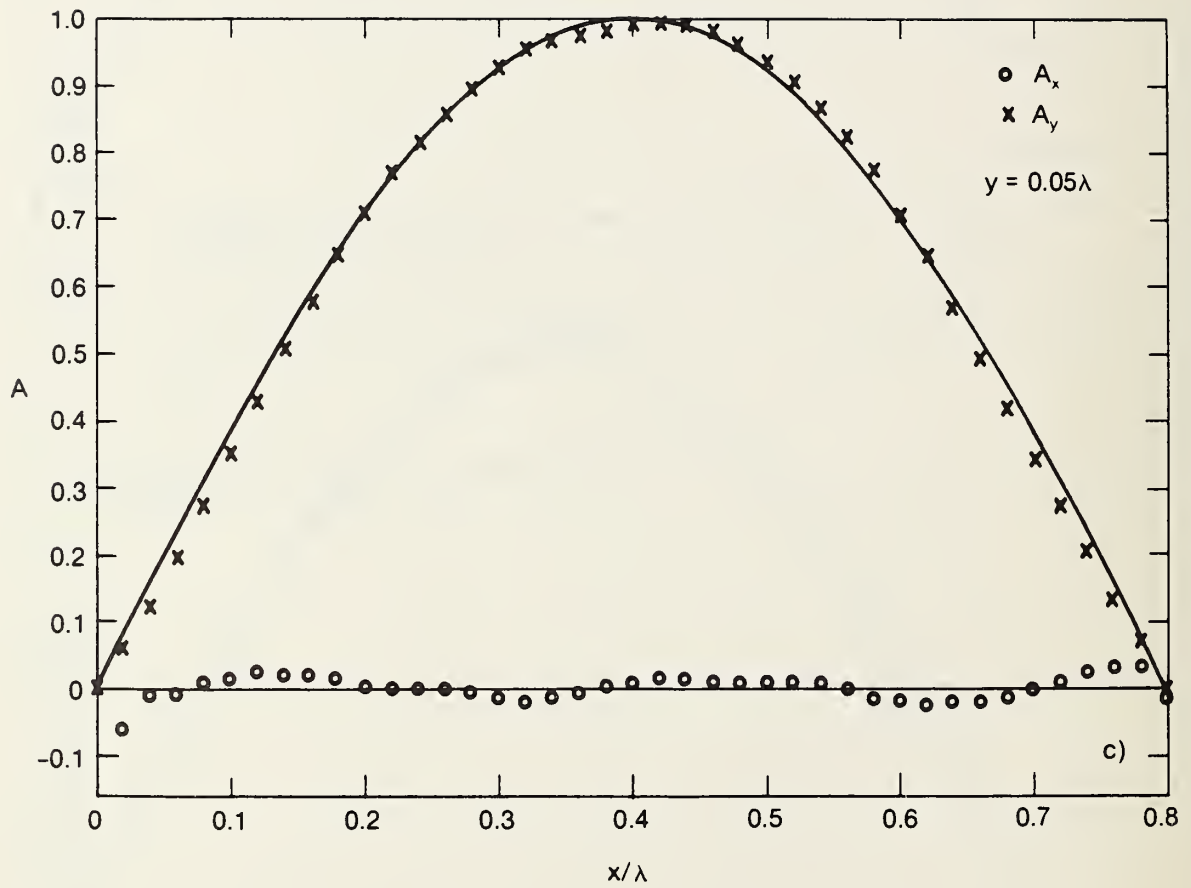


Figure 3-5. Fields A_x and A_y as functions of x at fixed y , after 65 passes through the grid in the numerical computation with nine measurement points. Solid line is correct result for A_y . Correct result for A_x is zero. a) $y = 0.2\lambda$ b) $y = 0.1\lambda$ c) $y = 0.05\lambda$



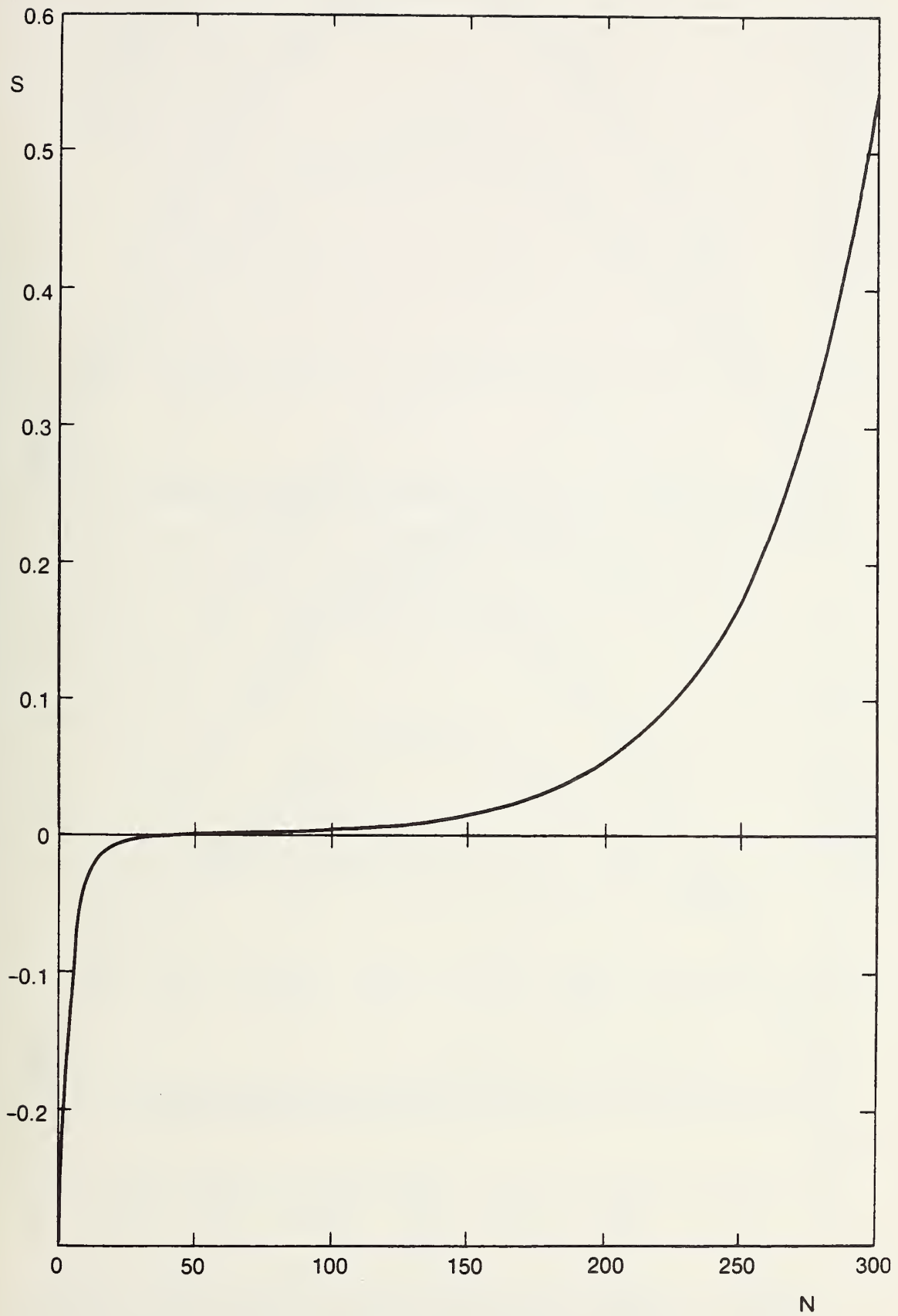


Figure 3-6. Action as function of N, for one measurement point.

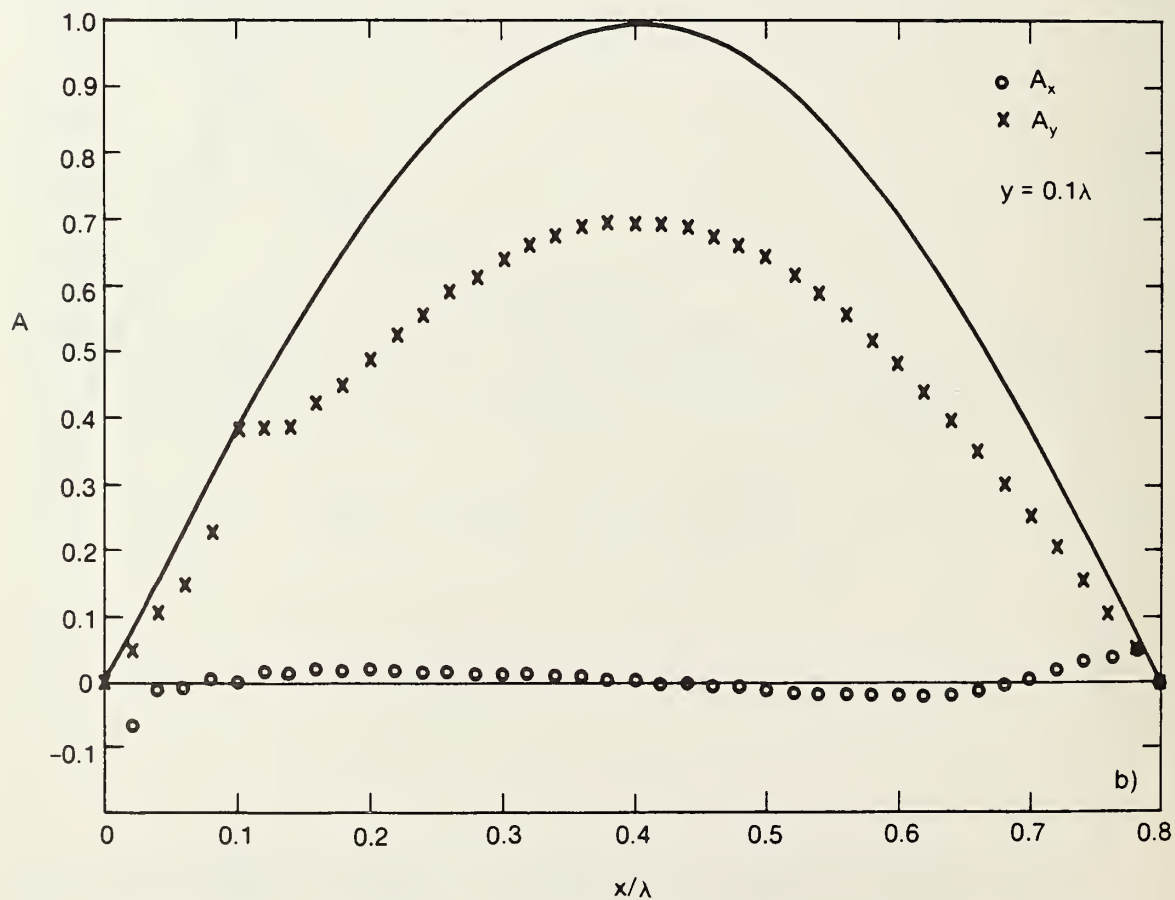
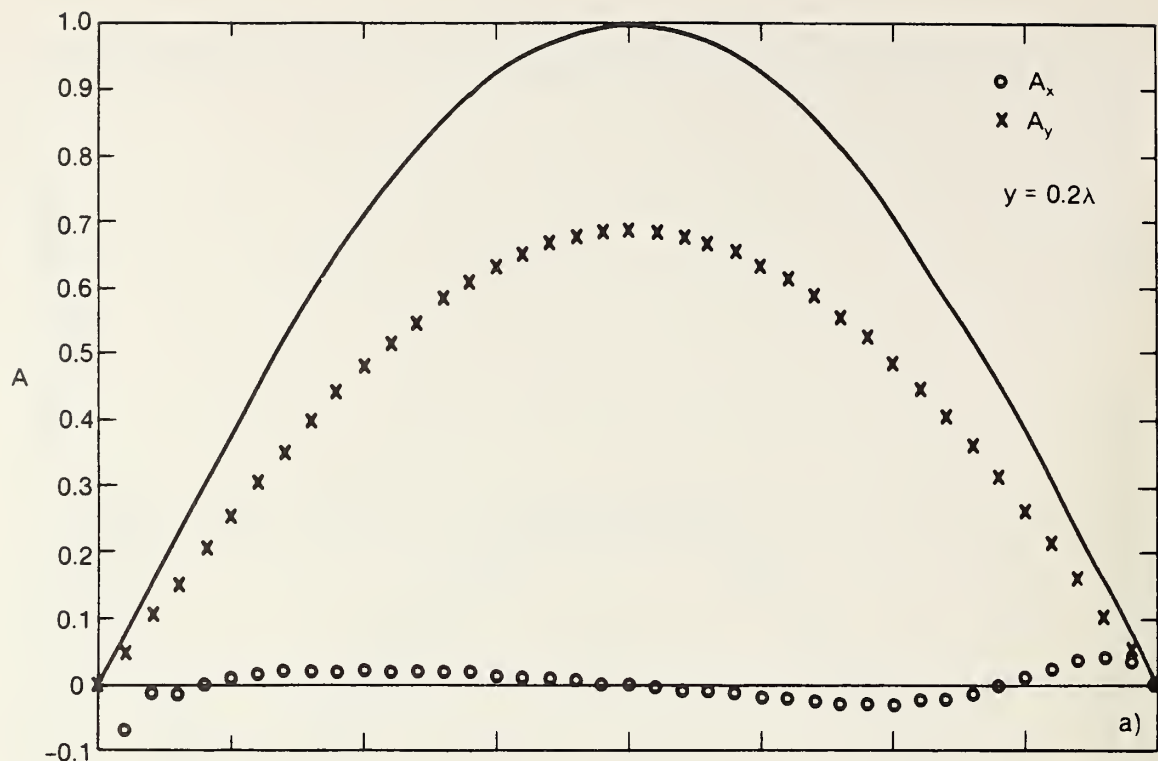
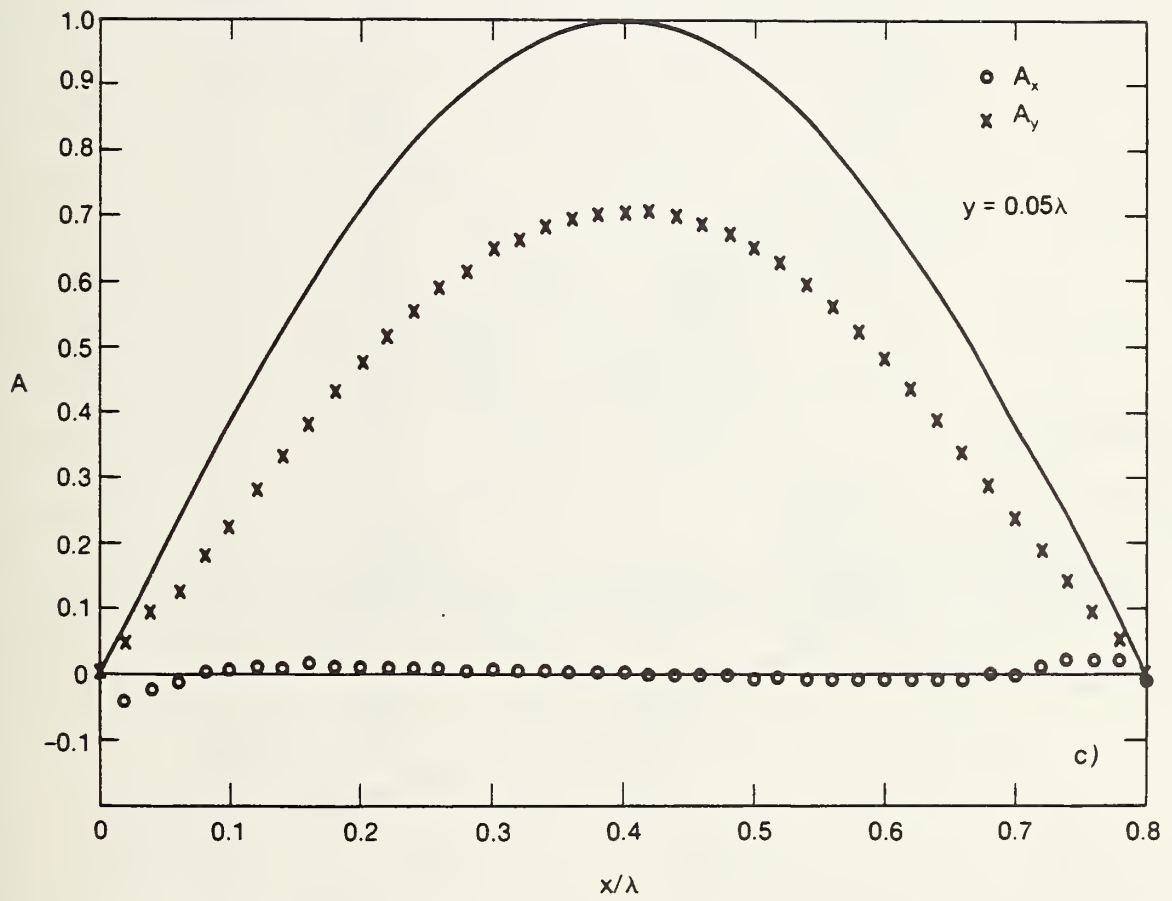


Figure 3-7. Computed fields as functions of x at fixed y , after 55 passes through the grid, with one measurement point. Solid line is correct result for A_y . Correct result for A_x is zero. a) $y = 0.2\lambda$ b) $y = 0.1\lambda$ c) $y = 0.05\lambda$



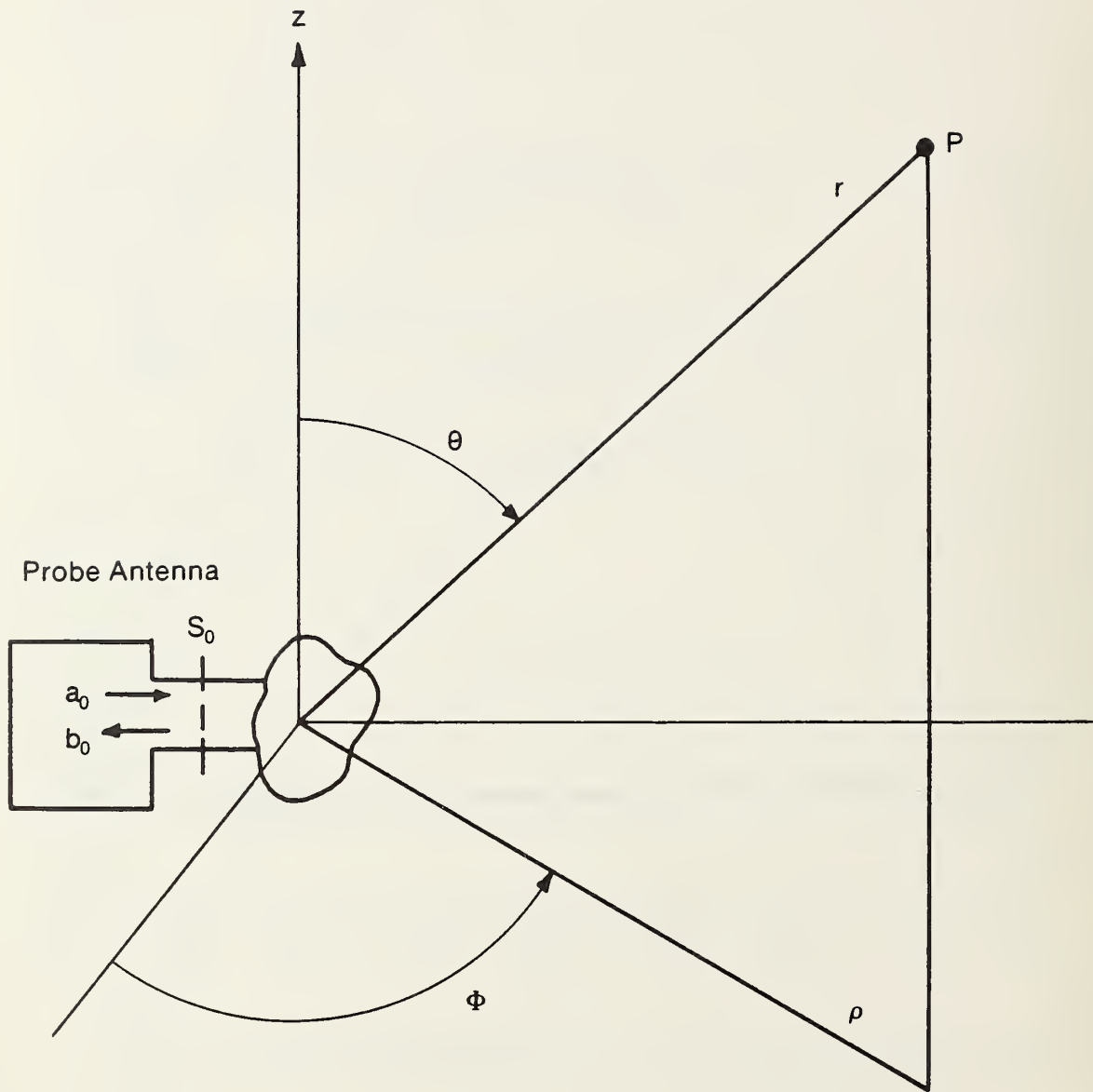


Figure 4-1. Coordinate system for probe antenna.

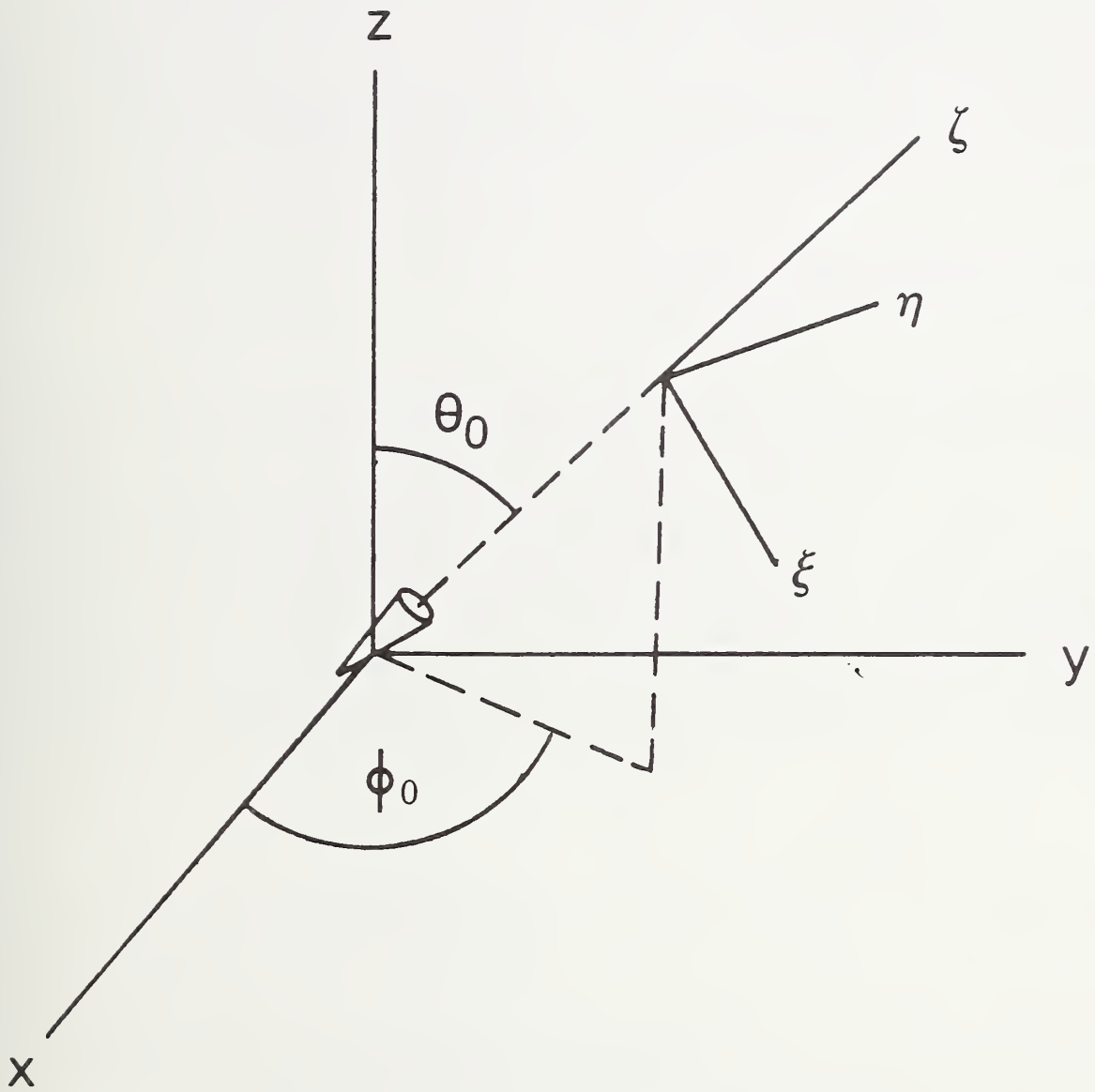


Figure 4-2. Coordinate-system conventions for spherical directional scanning.

U.S. DEPT. OF COMM. BIBLIOGRAPHIC DATA SHEET <i>(See instructions)</i>	1. PUBLICATION OR REPORT NO. NBS TN-1081	2. Performing Organ. Report No.	3. Publication Date March 1985
4. TITLE AND SUBTITLE Possible Estimation Methodologies for Electromagnetic Field Distributions in Complex Environments			
5. AUTHOR(S) M. Kanda, J. Randa and N. S. Nahman			
6. PERFORMING ORGANIZATION <i>(If joint or other than NBS, see instructions)</i> NATIONAL BUREAU OF STANDARDS DEPARTMENT OF COMMERCE WASHINGTON, D.C. 20234		7. Contract/Grant No.	8. Type of Report & Period Covered
9. SPONSORING ORGANIZATION NAME AND COMPLETE ADDRESS <i>(Street, City, State, ZIP)</i>			
10. SUPPLEMENTARY NOTES <input type="checkbox"/> Document describes a computer program; SF-185, FIPS Software Summary, is attached.			
11. ABSTRACT <i>(A 200-word or less factual summary of most significant information. If document includes a significant bibliography or literature survey, mention it here)</i> The problem of measuring and characterizing complicated multiple-source, multiple-frequency electromagnetic environments is becoming more important and more difficult as electrical devices proliferate. This paper outlines three general approaches to the problem which are currently under investigation at the National Bureau of Standards. The three approaches are: 1) a statistical treatment of the spatial distribution of electromagnetic field intensities, 2) a numerical computation using a finite-difference (or lattice) form of the electromagnetic action functional, and 3) use of a directional probe to scan a volume. All three methods are still in the development stage, but each appears promising.			
12. KEY WORDS <i>(Six to twelve entries; alphabetical order; capitalize only proper names; and separate key words by semicolons)</i> action, directional scanning, environment characterization, field levels, finite element, hazard assessment, multiple source, statistical approach			
13. AVAILABILITY <input checked="" type="checkbox"/> Unlimited <input type="checkbox"/> For Official Distribution. Do Not Release to NTIS <input checked="" type="checkbox"/> Order From Superintendent of Documents, U.S. Government Printing Office, Washington, D.C. 20402. <input type="checkbox"/> Order From National Technical Information Service (NTIS), Springfield, VA. 22161		14. NO. OF PRINTED PAGES 52	15. Price

NBS TECHNICAL PUBLICATIONS

PERIODICALS

JOURNAL OF RESEARCH—The Journal of Research of the National Bureau of Standards reports NBS research and development in those disciplines of the physical and engineering sciences in which the Bureau is active. These include physics, chemistry, engineering, mathematics, and computer sciences. Papers cover a broad range of subjects, with major emphasis on measurement methodology and the basic technology underlying standardization. Also included from time to time are survey articles on topics closely related to the Bureau's technical and scientific programs. As a special service to subscribers each issue contains complete citations to all recent Bureau publications in both NBS and non-NBS media. Issued six times a year. Annual subscription: domestic \$18; foreign \$22.50. Single copy, \$5.50 domestic; \$6.90 foreign.

NONPERIODICALS

Monographs—Major contributions to the technical literature on various subjects related to the Bureau's scientific and technical activities.

Handbooks—Recommended codes of engineering and industrial practice (including safety codes) developed in cooperation with interested industries, professional organizations, and regulatory bodies.

Special Publications—Include proceedings of conferences sponsored by NBS, NBS annual reports, and other special publications appropriate to this grouping such as wall charts, pocket cards, and bibliographies.

Applied Mathematics Series—Mathematical tables, manuals, and studies of special interest to physicists, engineers, chemists, biologists, mathematicians, computer programmers, and others engaged in scientific and technical work.

National Standard Reference Data Series—Provides quantitative data on the physical and chemical properties of materials, compiled from the world's literature and critically evaluated. Developed under a worldwide program coordinated by NBS under the authority of the National Standard Data Act (Public Law 90-396).

NOTE: The principal publication outlet for the foregoing data is the Journal of Physical and Chemical Reference Data (JPCRD) published quarterly for NBS by the American Chemical Society (ACS) and the American Institute of Physics (AIP). Subscriptions, reprints, and supplements available from ACS, 1155 Sixteenth St., NW, Washington, DC 20056.

Building Science Series—Disseminates technical information developed at the Bureau on building materials, components, systems, and whole structures. The series presents research results, test methods, and performance criteria related to the structural and environmental functions and the durability and safety characteristics of building elements and systems.

Technical Notes—Studies or reports which are complete in themselves but restrictive in their treatment of a subject. Analogous to monographs but not so comprehensive in scope or definitive in treatment of the subject area. Often serve as a vehicle for final reports of work performed at NBS under the sponsorship of other government agencies.

Voluntary Product Standards—Developed under procedures published by the Department of Commerce in Part 10, Title 15, of the Code of Federal Regulations. The standards establish nationally recognized requirements for products, and provide all concerned interests with a basis for common understanding of the characteristics of the products. NBS administers this program as a supplement to the activities of the private sector standardizing organizations.

Consumer Information Series—Practical information, based on NBS research and experience, covering areas of interest to the consumer. Easily understandable language and illustrations provide useful background knowledge for shopping in today's technological marketplace.

Order the above NBS publications from: Superintendent of Documents, Government Printing Office, Washington, DC 20402.

Order the following NBS publications—FIPS and NBSIR's—from the National Technical Information Service, Springfield, VA 22161.

Federal Information Processing Standards Publications (FIPS PUB)—Publications in this series collectively constitute the Federal Information Processing Standards Register. The Register serves as the official source of information in the Federal Government regarding standards issued by NBS pursuant to the Federal Property and Administrative Services Act of 1949 as amended, Public Law 89-306 (79 Stat. 1127), and as implemented by Executive Order 11717 (38 FR 12315, dated May 11, 1973) and Part 6 of Title 15 CFR (Code of Federal Regulations).

NBS Interagency Reports (NBSIR)—A special series of interim or final reports on work performed by NBS for outside sponsors (both government and non-government). In general, initial distribution is handled by the sponsor; public distribution is by the National Technical Information Service, Springfield, VA 22161, in paper copy or microfiche form.

U.S. Department of Commerce
National Bureau of Standards

Washington, D.C. 20234
Official Business
Penalty for Private Use \$300



POSTAGE AND FEES PAID
U.S. DEPARTMENT OF COMMERCE
COM-215

FIRST CLASS